FACULTY OF SCIENCE
UNIVERSITY OF COPENHAGEN

Strongly fluctuating spin systems

Anne Grosch

Niels Bohr Institute
University of Copenhagen
Jagtvej 155A, DK-2200, Copenhagen, Denmark

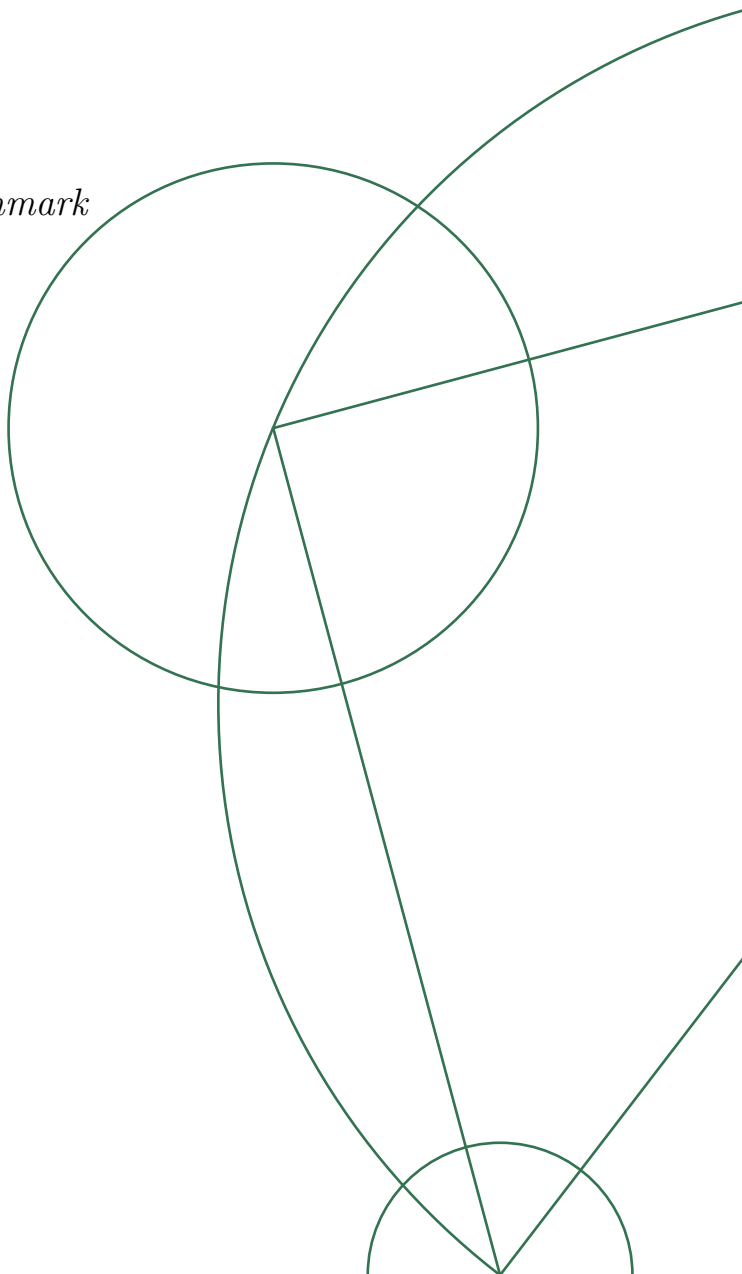

Master's Thesis in Physics

Supervisor: Jens Paaske

Dated: January 18, 2021

Abstract

The Heisenberg model on a two-dimensional square lattice with nearest and next-nearest neighbor exchange interactions exhibits a highly frustrated point at $J_2 = \frac{1}{2}|J_1|$. Introducing spin-waves into this system in both a classical and a quantum mechanical (Holstein-Primakoff) spin-wave theory yields a spin-wave dispersion relation at the highly frustrated point. At this point the dispersion has a whole spectrum of zero-energy modes, which indicates that faulty assumptions have been used in the calculation. This thesis investigates whether adding additional interactions to the system will correct the issues of the spin-wave dispersion. The square lattice is stretched to an orthorhombic lattice, where the exchange interactions differ in the two perpendicular directions of the lattice. The ground state spin configuration of this lattice is determined and spin-waves are introduced into the system. By stretching the square lattice, the symmetries of the system are reduced which subsequently lead to a reduction of zero-energy modes in the spin-wave dispersion, as the highly frustrated point does not exist in the orthorhombic lattice. Thereafter the anisotropic Dzyaloshinsky-Moriya interaction on the two-dimensional square lattice is added to the J_1-J_2 Heisenberg model. The ground state spin configuration is determined using the Luttinger-Tisza method, and the possibility of adding an external magnetic field is considered. Once more spin-waves are introduced, and the spin-wave dispersion relation is determined using a classical and a quantum mechanical spin-wave theory, and the relations are found to be in agreement. This spin-wave dispersion only contains a zero-energy mode at the Γ-point. Both additional interactions reduce the amount of zero-energy modes in the spin-wave dispersion.

Acknowledgments

First and foremost I would like to extend my thanks to my supervisor Jens Paaske for his tireless help and patience during the making of this thesis and most importantly for teaching me to evaluate $\cos(\pi)$. I am thankful to have been able to complete both my Bachelor and Master thesis in cooperation with Jens and the CMT group, and I appreciate the interesting discussions we have had.

My friends and family deserve endless praise for their unwavering support and patience, through global pandemics and lockdowns of society, especially towards the end of the process of writing this thesis. Particularly Freja and Cecilie have been the best office mates one could wish for, always ready to answer questions and offer support. A special thanks goes out to Anton and Lasse for proofreading and offering valuable commentary.

Contents

Chapter 1

Introduction

Materials, which are characterized as magnetic, contain an array of magnetic moments arranged in a lattice. These magnetic moments may arrange themselves in a multitude of different ways, enabling a multitude of different structures and characteristics; one of which being the phenomenon of frustration. A magnetic system containing frustration is one in which all competing interactions cannot be satisfied simultaneously, may it be geometric frustration, where the geometry of the lattice prevents all interactions from minimizing simultaneously, or frustration through interaction, to which long-range exchange interactions is the most common cause. Frustration of magnetic systems leads to an extensive degeneracy of the ground state. Systems containing frustration are of great interest as they can lead to the manifestation of a multitude of different fascinating phenomena. They are for example thought to play an important part in the understanding of unconventional superconductors [1, 2].

The interaction between periodic arrays of spins can be modeled by the Heisenberg model, where the interaction between two spins at site i and j are characterized by the exchange interaction J_{ij}. Frustration through interaction is effortlessly obtained when adding long-range interactions, as it quickly becomes difficult to satisfy conflicting interactions on all lattice geometries when interactions reach farther than the closest neighbor to a given site. Just two interactions are enough to create frustration, which the J_1-J_2 Heisenberg model is an excellent example of. This seemingly simple model manifests several complex theoretical concepts. In this model, an atom interacts with its nearest and next-nearest neighbors through J_1 and J_2, respectively. On the square lattice, the ground state spin configuration is unsurprisingly a simple ferromagnet or antiferromagnet, depending on the sign of the nearest neighbor interaction, for weak next-nearest neighbor interactions, $J_2 < |J_1|$. For $J_2 > |J_1|$, however, the system exhibits frustration as the ground state spin configuration consists of two interpenetrating Néel lattices differing by an arbitrary relative angle. A point of particular interest is at $J_2 = \frac{1}{2}|J_1|$ as this makes the system highly frustrated, and no magnetic order is exhibited as a result.

According to the Mermin-Wagner theorem, no spontaneous breaking of a continuous symmetry can occur at finite temperature in the two-dimensional model; however, the system shows a discrete nematic phase transition at finite temperature [3]. Close to the highly frustrated point, the system is thought to form a spin liquid [4, 5]. Furthermore, when spin-waves are considered at the highly frustrated point the resulting spin-wave dispersion gives rise to a whole spectrum of zero-energy modes. This indicates the possibility of faulty assumptions having been used in the calculation. This thesis investigates the possibility of this discrepancy being fixed by adding additional interactions to the model, namely considering an orthorhombic lattice and adding an anisotropic exchange interaction.

The orthorhombic lattice describes a system in which the spacing is different in the two perpendicular directions of the lattice. This means that the "nearest neighbor" interaction differs in these directions, and might instead be described by a J_{1y}-J_{1z}-J_2 Heisenberg model on the two-dimensional lattice in the yz-plane. J_2 then actually describes the third nearest neighbor coupling, and an additional interaction has therefore been added. This is minor change to the geometry of the system, but it changes the fluctuation spectrum when spin-waves are considered.

The other additional interaction which will be considered in this thesis is the anisotropic exchange interaction, which stems from considering the spin-orbit coupling in Anderson theory of superexchange [6]. The interaction was first formulated by Dzyaloshinsky and Moriya [7, 8] and is therefore called the Dzyaloshinksy-Moriya (DM) interaction. This interaction couples the cross product of the classical spin vectors through the exchange vector $\mathbf{D}_{ij}$ between site i and j, which depends on the lattice geometry. The DM interaction is thought to be a source of stabilized skyrmions [9, 10], which are candidates for spintronic devices, where the spin of electron is exploited as an additional degree of freedom compared to regular electronics. The DM interaction is present in systems such as copper formate tetradeuterate (CFTD), which is close to an ideal two-dimensional Heisenberg antiferromagnet with nearest neighbor exchange constant $J = 6.3$meV and DM interaction strength $d = 0.46$meV [11].

The purpose of this thesis is, thus, to investigate the behavior of different systems under collective spin excitations and to see the change relative to the highly frustrated J_1-J_2 Heisenberg model, in which the spin-wave theory describes an unphysical system.

1.1 Outline of thesis

The thesis is structured in the following way to give an in-depth introduction to the system which constitutes the starting point of the investigation, the J_1-J_2 Heisenberg

model on a square lattice. Subsequently, alterations are added, and the effect they have on the original setup is determined.

- An overview of relevant background material necessary for the following chapters is contained in Chapter 2.
- In Chapter 3, the ground state spin configuration of the J_1-J_2 Heisenberg model is found and is subsequently subjected to spin fluctuations using both a classical and a quantum mechanical spin-wave theory. The spin-wave dispersion relation is determined and is found to be the same in the two theories.
- In Chapter 4, he square lattice model is generalized to the orthorhombic J_{1y}-J_{1z}-J_2 Heisenberg model and the effect that the stretching of the lattice has on the spin-wave dispersion is discovered.
- In Chapter 5, the asymmetric Dzyaloshinsky-Moriya interaction is added to the J_1-J_2 Heisenberg model, and the ground state spin configuration and spin-wave dispersion are determined. Once again, the same expression for the dispersion is obtained using both a classical and a quantum mechanical spin-wave theory as a way of verifying the relation.
- Chapter 6 presents conclusions and discusses potential options for future research on the subjects of this thesis.

Chapter 2

Background

2.1 Magnetic materials

Solid magnetic materials contain microscopic magnetic moments, spins, arranged in a periodic crystalline structure. They arrange themselves in such a manner as it is the simplest way that the atoms can be arranged to create a macroscopic solid [12]. One explanation for them being periodic might be that if a certain arrangement lowers the energy in the vicinity of one atom, the same arrangement probably does so for similar atoms. This periodic arrangement can have endless compositions but a certain subgroup of these structures are the so-called Bravais lattices. These are lattices where all points within it are equivalent and can be described by

$$\mathbf{r} = n\mathbf{a}_1 + m\mathbf{a}_2 \tag{2.1}$$

in two dimensions, where $\mathbf{a}_1$ and $\mathbf{a}_2$ are the two-dimensional primitive lattice vectors and n and m are integers. Note that the choice of lattice vectors is not unique and can be determined in several different ways. The square and the rectangular lattices are examples of Bravais lattices in two dimensions. However far from all materials in nature can be characterized by Bravais lattices, and those who cannot are called non-Bravias lattices. In the non-Bravais lattice not all point are equivalent, and they can be characterized by two (or more) interpenetrating Bravais lattices. An example of a non-Bravais lattice is the honeycomb lattice.

The real-space lattice associates each atom with a position in the lattice structure, but materials are also defined through their reciprocal lattice. The reciprocal lattice is similarly characterized by reciprocal lattice vectors. One can move between real space and $\mathbf{q}$-space using Fourier transformations. The first Brillouin Zone is spanned by the Wigner-Seitz cell around the origin in reciprocal space. The reciprocal lattice is periodic and it is therefore sufficient to explore the first Brillouin Zone when performing sums or integrals over $\mathbf{q}$.

In reciprocal space the so-called star of $\mathbf{Q}$ can be defined. The star of $\mathbf{Q}$ is the set of discrete non-equivalent values of $\mathbf{Q}$ in the first Brillouin Zone [13]. Two $\mathbf{q}$-vectors are said to be equivalent if their difference constitutes a reciprocal lattice vector. $\mathbf{Q}$ is a $\mathbf{q}$-vector which minimizes the exchange interactions.

2.2 Magnetic interactions

The magnetic moments in the lattice structures of crystalline materials interact with each other through numerous different interactions. These magnetic moments may interact to induce long range (or short range) order in the system. The interactions can be modeled by different theories. The most relevant models are discussed in the following sections.

2.2.1 Magnetic dipole-dipole interaction

One type of interaction is the magnetic dipole interaction. The interaction between two magnetic dipoles μ_1 and μ_2, separated by displacement $\mathbf{r}$, is given by [14]

$$E = \frac{\mu_0}{4\pi r^3}\left[\mu_1 \cdot \mu_2 - \frac{3}{r^2}\left(\mu_1 \cdot \mathbf{r}\right)\left(\mu_2 \cdot \mathbf{r}\right)\right] . \tag{2.2}$$

However this interaction is too weak, even when two magnetic dipoles are separated by typical distances at the atomic scale, to explain ordering in most magnetic materials [12]. The effect of the magnetic dipole-dipole is therefore often negligible when considering small-scale phenomena.

2.2.2 Exchange interaction

The interaction between the spin angular momenta of two particles can be modeled after the Heisenberg model

$$H = \frac{1}{2}\sum_{ij} J_{ij}\mathbf{S}_i \cdot \mathbf{S}_j \tag{2.3}$$

where i and j refer to lattice sites and $\mathbf{S}_{i,j}$ is the spin operator at site i, j. J_{ij} is the exchange constant between two sites, and it decays exponentially with the distance between the two sites as it depends on the degree of overlap of the the atomic wave functions. The factor $\frac{1}{2}$ accounts for double counting of the coupled lattice sites.

The sign and magnitude of the exchange constant determines the ground state spin configuration in a given system. Consider for example a two-dimensional square lattice with exchange constant $J_{ij} = J$ for i, j being nearest neighboring lattice sites and $J_{ij} = 0$ otherwise. On the other hand for $J < 0$ the system would assume a ferromagnetic configuration, where all neighboring spins are aligned. For $J > 0$ the configuration would

be antiferromagnetic, where all spins are anti-aligned. This example is very simple and intuitively clear. However, as it often is with physics, this is not always the case. Adding a non-zero exchange interaction between next-nearest or even next-next-nearest neighboring sites complicates the case and makes the ground state configuration a result of the competition between the strenghts of these different interactions, which can all be both ferromagnetic or antiferromagnetic. The lattice configuration might also complicate the case further. Consider for example a two-dimensional triangular lattice with antiferromagnetic nearest neighbor exchange interaction, see Fig. (2.1). The energy will be minimized when the spins are anti-aligned, but the structure of the lattice prevents all sites from anti-aligning with their nearest neighbor. The system is then frustrated, as there is no single, unique ground state spin configuration, as one of the antiferromagnetic interactions in the triangle will always be unattained. The ground state spin configuration turns out to be one where the spins are rotated by 120° relative to their neighbors [15].

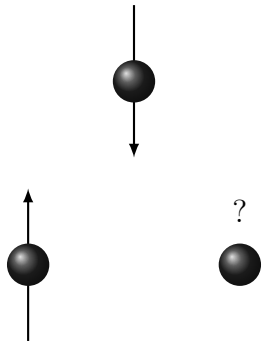

Figure 2.1: Triangular lattice with antiferromagnetic nearest neighbor exchange constant resulting in a frustrated system, as all 3 spins cannot simultaneously anti-align.

2.2.3 Anisotropic exchange interaction

Another type of exchange interaction is the anisotropic exchange interaction, also sometimes called the antisymmetric exchange interaction. The typical form of this interaction is

$$H = \sum_{ij} \mathbf{D}_{ij} \cdot (\mathbf{S}_i \times \mathbf{S}_i) \ , \tag{2.4}$$

where $\mathbf{D}_{ij}$ is the antisymmetric exchange vector which depends on the geometry of the lattice. The existence of this interaction was first discussed by Dzyaloshinsky [7] and later formally formulated by Moriya [8], and it is therefore referred to as the Dzyaloshinsky-Moriya interaction. The symmetric exchange interaction has lowest energy when the spins are either aligned or anti-aligned, while the antisymmetric exchange interaction favors spins at a right angle in a plane perpendicular to $\mathbf{D}$. Hence when both interactions are present there will be a competition between these two interactions. When only the

DM interaction is present the effect will be to slightly rotate the spins by a small angle, leading to the phenomenon of weak ferromagnetism [8].

The shape of the antisymmetric exchange vector $\mathbf{D}_{ij}$ coupling two atoms at location i and j respectively can be determined from the following set of rules [8]. Denote the point bisecting the straight line ij by k, see Fig. (2.2). Then

1. When a center of inversion is at k, the exhcange vector is $\mathbf{D}_{ij} = 0$.
2. When a mirror plane $\perp ij$ passes through k, $\mathbf{D}_{ij} \parallel$ to the mirror plane or $\mathbf{D}_{ij} \perp ij$.
3. When there is a mirror plane including i and j, $\mathbf{D}_{ij} \perp$ to the mirror plane.
4. When a two-fold rotation axis $\perp$ to ij passes through k, $\mathbf{D}_{ij} \perp$ to the two-fold axis.
5. When there is an n-fold axis (where $n \geq 2$) along ij, $\mathbf{D}_{ij} \parallel ij$.

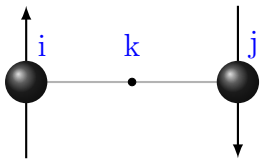

Figure 2.2: Two lattice points at locations i and j with point k bisecting the line connecting them.

2.3 Weak and local constraint

Magnetism is purely a quantum mechanical effect, as the Bohr-van Leeuwen theorem states, since the thermal average of the magnetization is zero within classical statistical mechanics. However magnetism can be explored in a classical manner by treating the effective spins of atoms as classical vectors in the large spin limit. These classical spins can be treated under the local constraint

$$|\mathbf{S}_i|^2 = S^2 \,. \tag{2.5}$$

But to minimize the energy under this constraint using the Luttinger-Tisza method [16] would require $\mathcal{N}$ site dependent Lagrange multipliers λ_i, where $\mathcal{N}$ is the amount sites in the lattice. So to make things simpler the local constraint is often relaxed to the weak constraint

$$\sum_i |\mathbf{S}_i|^2 = \mathcal{N} S^2 \tag{2.6}$$

stating that only the average of the spins is conserved, and not every single spin, as in Eq. (2.5). To minimize the energy under the weak constraint using Lagrange multipliers

would only require a single Lagrange multiplier λ, hence the situation has been simplified significantly. It is clear that the spins obeying the weak constraint in Eq. (2.6) make up a subset of the spins already obeying the local constraint.

2.4 Fourier conventions

In this thesis the following conventions for the discrete Fourier transform and inverse discrete Fourier transform of classical spin vectors will be used

$$\mathbf{S}_i = \frac{1}{\sqrt{\mathcal{V}}} \sum_{\mathbf{q}} \mathrm{e}^{i\mathbf{q}\cdot\mathbf{r}_i}\, \mathbf{S}_{\mathbf{q}} \tag{2.7}$$

$$\mathbf{S}_{\mathbf{q}} = \frac{1}{\sqrt{\mathcal{V}}} \sum_{i} \mathrm{e}^{-i\mathbf{q}\cdot\mathbf{r}_i}\, \mathbf{S}_i \,. \tag{2.8}$$

The convention is completely analogous to Eq. (2.7) and Eq. (2.8) for Fourier transforms of other types of operators used, such as Holstein-Primakoff bosons and π-fields.

The Fourier transform of exchange interactions is defined a bit differently, as the Heisenberg exchange constant used in this thesis is

$$J_{ij} = \frac{1}{\mathcal{V}} \sum_{\mathbf{q}} \mathrm{e}^{i\mathbf{q}\cdot\boldsymbol{\delta}_{ij}}\, J_{\mathbf{q}} \tag{2.9}$$

$$J_{\mathbf{q}} = \sum_{\boldsymbol{\delta}_{ij}} \mathrm{e}^{-i\mathbf{q}\cdot\boldsymbol{\delta}_{ij}}\, J_{ij} \,, \tag{2.10}$$

where $\boldsymbol{\delta}_{ij} = (\mathbf{r}_i - \mathbf{r}_j)$. The Fourier transfrom of the Dzyaloshinsky-Moriya exchange vector is

$$\mathbf{D}_{ij} = \frac{1}{\mathcal{V}} \sum_{\mathbf{q}} \mathrm{e}^{i\mathbf{q}\cdot\boldsymbol{\delta}_{ij}}\, \mathbf{D}_{\mathbf{q}} \tag{2.11}$$

$$\mathbf{D}_{\mathbf{q}} = \sum_{\boldsymbol{\delta}_{ij}} \mathrm{e}^{-i\mathbf{q}\cdot\boldsymbol{\delta}_{ij}}\, \mathbf{D}_{ij} \,. \tag{2.12}$$

Additionally the very useful relation between a sum of complex exponential functions and the Dirac delta function is applied numerous times according to the following definition

$$\frac{1}{\mathcal{V}} \sum_{\mathbf{q}} \mathrm{e}^{i\mathbf{q}\cdot\mathbf{r}_i} = \delta(\mathbf{r}_i) \,. \tag{2.13}$$

Chapter 3

The Heisenberg model

This chapter contains a classification of the Heisenberg model along with the determination of the ground state spin configuration in the J_1-J_2 model on a two-dimensional square lattice. The frustration of the ground state is discussed and spin fluctuations are introduced into the system. The spin-wave dispersion is determined using both a classical and a quantum mechanical spin-wave theory. This chapter is based on [16] and [17].

3.1 Ground state spin configuration

The general Heisenberg model is given by

$$H = \frac{1}{2}\sum_{ij} J_{ij}\mathbf{S}_i \cdot \mathbf{S}_j \tag{3.1}$$

where $\mathbf{S}_i$ is the spin on the atom at site i in the lattice and J_{ij} is the Heisenberg exchange interaction between the atoms at site i and site j. The Heisenberg exchange interaction is translationally and reflectionally symmetric and, as discussed in the previous chapter, it is trivial that $J_{ij} < 0$ ($J_{ij} > 0$) favors alignment (anti-alignment) of spins $\mathbf{S}_i$ and $\mathbf{S}_j$ when treated as classical vectors.

Minimizing the energy while imposing the weak constraint $\sum_i |\mathbf{S}_i|^2 = \mathcal{N}S^2$ yields a set of equations

$$0 = \frac{\partial}{\partial S_i^\alpha}\left[\frac{1}{2}\sum_{ij} J_{ij}\mathbf{S}_i \cdot \mathbf{S}_j - \lambda\left(\sum_i |\mathbf{S}_i|^2 - \mathcal{N}S^2\right)\right] \tag{3.2}$$

for $\alpha \in \{x, y, z\}$. λ is a Lagrange multiplier, of which only one is needed according to Sec. (2.3). This stationary condition yields the set of eigenvalue equations

$$\frac{1}{2}\sum_j J_{ij}S_j^\alpha = \lambda S_i^\alpha \,. \tag{3.3}$$

These equations have eigenvalue $\lambda = \frac{1}{2}J_{\mathbf{Q}}$ and are solved by

$$S_i^\alpha = A_\alpha \cos\left(\mathbf{Q}\cdot\mathbf{r}_i + \phi_\alpha\right) \tag{3.4}$$

for real phases ϕ_α, which can be shown by

$$\begin{aligned}\frac{1}{2}\sum_j J_{ij}S_j^\alpha &= \frac{1}{2}\sum_j J_{ij}A_\alpha \cos\left(\mathbf{Q}\cdot\mathbf{r}_j + \phi_\alpha\right) \\ &= \frac{1}{4\mathcal{V}}\sum_{\mathbf{q}}\sum_j A_\alpha J_{\mathbf{q}} \mathrm{e}^{i\mathbf{q}\cdot(\mathbf{r}_i-\mathbf{r}_j)}\left(\mathrm{e}^{i(\mathbf{Q}\cdot\mathbf{r}_j+\phi_\alpha)} + \mathrm{e}^{-i(\mathbf{Q}\cdot\mathbf{r}_j+\phi_\alpha)}\right) \\ &= \frac{1}{2}J_{\mathbf{Q}}A_\alpha\cos\left(\mathbf{Q}\cdot\mathbf{r}_i+\phi_\alpha\right)\end{aligned} \tag{3.5}$$

where the Fourier transform of the Heisenberg exchange interaction, given by Eq. (2.9), was inserted, and the fact that $J_{-\mathbf{Q}} = J_{\mathbf{Q}}$ was utilized. The ground state spins satisfying the weak constraint thus comprises planar spiral, and it is composed of a single $\mathbf{q}$-vector. The energy of the system is

$$E = \frac{1}{2}\mathcal{N}J_{\mathbf{Q}} \tag{3.6}$$

where $\mathcal{N}$ is the total number of sites in the lattice. $\mathbf{Q}$ may be chosen to minimize the energy, which is done by choosing the $\mathbf{q}$-vector which minimizes $J_{\mathbf{q}}$.

The fulfillment of the local constraint rather than the weak constraint can be met by adjusting the free parameters of S_i^α. Choosing two of the constants A^α to be 1 and the remaining to be 0, while the one of the phases is $\phi_\alpha = \phi$ and the other one is $\phi_\alpha = \phi + \frac{\pi}{2}$ is one way of doing this. The spin configuration then becomes

$$\mathbf{S}_i = \cos\left(\mathbf{Q}\cdot\mathbf{r}_i+\phi\right)\hat{\boldsymbol{u}} + \sin\left(\mathbf{Q}\cdot\mathbf{r}_i+\phi\right)\hat{\boldsymbol{v}}\,. \tag{3.7}$$

The unit vectors $\hat{\boldsymbol{u}}$ and $\hat{\boldsymbol{v}}$ may be pointed in any direction where $\hat{\boldsymbol{u}} \perp \hat{\boldsymbol{v}}$. For simplicity the phase ϕ is $\phi = 0$ henceforth.

3.1.1 J_1-J_2 model on two-dimensional square lattice

The J_1-J_2 model is used to describe a system where each atom is coupled to their nearest (next-nearest) neighbor via the exchange interaction J_1 (J_2). In the two-dimensional square lattice each atom is positioned at a site i in the lattice, described by

$$\mathbf{r}_i = n_i\mathbf{a}_1 + m_i\mathbf{a}_2 \tag{3.8}$$

where $\mathbf{a}_{1,2}$ are the primitive lattice vectors and $n_i, m_i \in \mathbb{Z}$. The rectangular lattice is an example of such a system, and the primitive lattice vectors depend on the lattice constants. For the rectangular lattice in the yz-plane one choice of primitive lattice vectors

is $\mathbf{a}_1 = (a_1^y, a_1^z)^{\mathrm{T}} = (a_y, 0)^{\mathrm{T}}$ and $\mathbf{a}_2 = (0, a_z)^{\mathrm{T}}$, see Fig. (3.1). In the following section the square lattice, where $a_y = a_z$ will be treated, while the orthorhombic lattice, with $a_y \neq a_z$ will be investigated in Sec. (4).

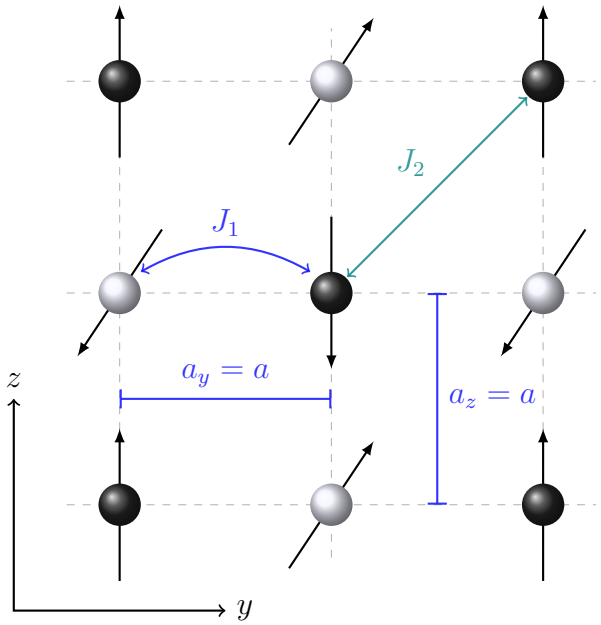

Figure 3.1: The two-dimensional square lattice ground state spin configuration in the J_1-J_2 Heisenberg model with two antiferromagnetic sublattices represented by white and black points, nearest (next-nearest) neighbor exchange constant J_1 (J_2) and lattice constants $a_y = a_z$.

In the square lattice the four nearest neighbors of site i are situated at lattice sites $\mathbf{r}_i \pm a\hat{\boldsymbol{y}}$ and $\mathbf{r}_i \pm a\hat{\boldsymbol{z}}$ and the four next-nearest neighbors are situated diagonally at $\mathbf{r}_i \pm a\hat{\boldsymbol{y}} \pm a\hat{\boldsymbol{z}}$. The system is described by the Heisenberg Hamiltonian given by Eq. (2.3). Upon inserting the Fourier transform of the spins, given by Eq. (2.7), the Hamiltonian assumes the form

$$H = \frac{1}{2} \sum_{\mathbf{q}} J_{\mathbf{q}} \mathbf{S}_{\mathbf{q}} \cdot \mathbf{S}_{-\mathbf{q}} \tag{3.9}$$

where

$$J_{\mathbf{q}} = 2J_1 \left(\cos\left(q_y a\right) + \cos\left(q_z a\right)\right) + 4J_2 \cos\left(q_y a\right) \cos\left(q_z a\right) \ . \tag{3.10}$$

By minimizing the energy, corresponding to minimization of $J_{\mathbf{q}}$ with respect to $\mathbf{q}$, it is apparent that the appropriate minima $\mathbf{Q} = (Q_y, Q_z)$ depends on the strength of the exchange interactions between sites. There are two straightforward cases; for $J_1, J_2 < 0$ both the nearest and next-nearest neighbor couplings prefer alignment of the spins, and the energy is minimized by $\mathbf{Q} = (0, 0)$ simply resulting in a completely ferromagnetic system. For $J_1 > 0$, $J_2 < 0$ the couplings are also not conflicting and energy is minimized by $\mathbf{Q} = \frac{1}{a}(\pi, \pi)$, resulting in an antiferromagnetic system. In both of these cases the star of $\mathbf{Q}$ only contains one element, and the ground state spin configuration is therefore

described by Eq. (3.7).

However when $J_2 > 0$ the nearest and next-nearest neighbor couplings cannot be satisfied simultaneously and a competition to dominate arises between them, making the system frustrated. For $J_2 < \frac{1}{2}|J_1|$ the interaction is dominated by the nearest neighbor coupling, and the minimum is at $\mathbf{Q} = \frac{1}{a}(\pi, \pi)$ ($\mathbf{Q} = (0, 0)$), see Fig. (3.2a), if J_1 prefers anti-alignment (alignment) of the spins. Once again the spin configuration is given by Eq. (3.7). For $J_2 > \frac{1}{2}|J_2|$ there is a transition to either $\mathbf{Q}^{(1)} = \left(0, \frac{\pi}{a}\right)$ or $\mathbf{Q}^{(2)} = \left(\frac{\pi}{a}, 0\right)$, see Fig. (3.2b).

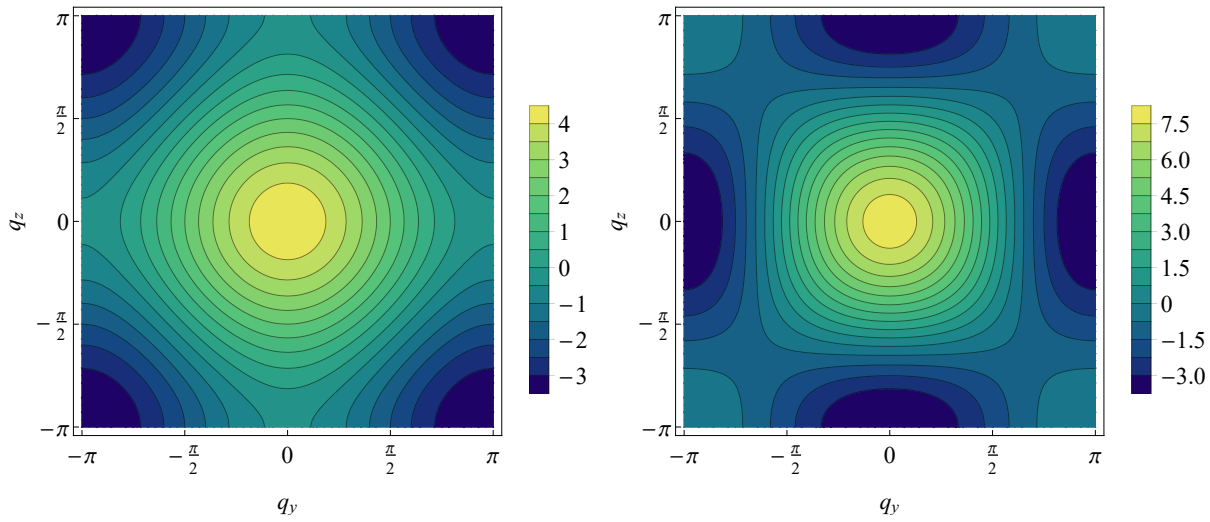

(a) $J_{\mathbf{q}}$ for $J_1 = 1$, $J_2 = 0.1$.

(b) $J_{\mathbf{q}}$ $J_1 = 1$, $J_2 = 1$.

Figure 3.2: Contour plot of $J_{\mathbf{q}}$ from Eq. (3.10) for different strengths of the exchange interaction J_1 (J_2) between nearest (next-nearest) neighboring sites in the two-dimensional square lattice with $a = 1$. The minimum of $J_{\mathbf{q}}$ shifts from $(Q_y, Q_z) = \frac{1}{a}(\pi, \pi)$ to $\mathbf{Q}^{(1)} = \left(0, \frac{\pi}{a}\right)$ or $\mathbf{Q}^{(2)} = \left(\frac{\pi}{a}, 0\right)$ as J_2 increases from $J_2 < \frac{1}{2}|J_1|$ to $J_2 > \frac{1}{2}|J_1|$.

When $J_2 > \frac{1}{2}|J_1|$ the star of $\mathbf{Q}$ contains two elements $\mathbf{Q}^{(1)}$ and $\mathbf{Q}^{(2)}$. Since $2\mathbf{Q}$ is a reciprocal lattice vector for both of these $\mathbf{q}$'s, the ground state spin configuration can be described by [13]

$$\mathbf{S}_i = \cos\left(\varphi_i^{(1)}\right)\cos(\Theta)\hat{\boldsymbol{u}} + \cos\left(\varphi_i^{(2)}\right)\sin(\Theta)\hat{\boldsymbol{v}} \tag{3.11}$$

where $\varphi_i^{(1)} = \mathbf{Q}^{(1)} \cdot \mathbf{r}_i$ and $\varphi_i^{(2)} = \mathbf{Q}^{(2)} \cdot \mathbf{r}_i$. The unit vectors $\hat{\boldsymbol{u}} \perp \hat{\boldsymbol{v}}$. Hence the spin configuration is split up into two interpenetrating Néel sublattices, see Fig. (3.1), where sites belonging to one sublattice are represented by white circles and sites belonging to the other are represented by black circles. $2\Theta = \theta$ represents the angular separation between the two sublattices. In this case the ground state energy of the system is $E = -2\mathcal{N}J_2$. It is therefore evident that ground state energy is independent of the orientation of the sublattices, since there is no dependency on the angle Θ, and the system is therefore

degenerate in this angle.

In between these two cases there is the situation of $J_2 = \frac{1}{2}|J_1|$, where $\mathbf{Q}$ actually is every point on the entire edge of the Brillouin Zone, see Fig. (3.3).

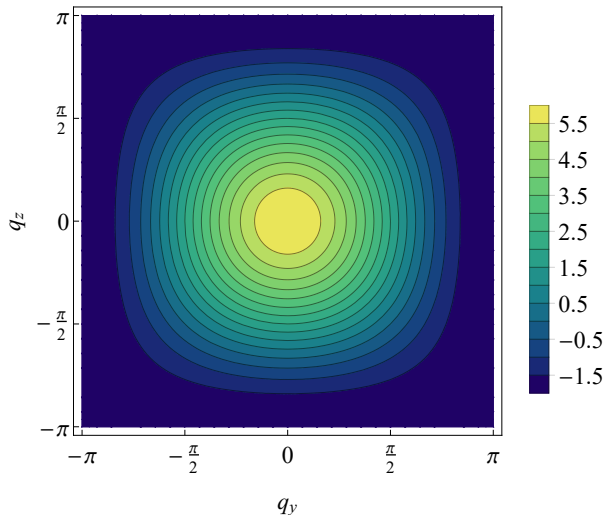

Figure 3.3: Contour plot of exchange interaction $J_{\mathbf{q}}$ in the two-dimensional square lattice with $a = 1$ for $J_1 = 1$, $J_2 = 0.5$.

3.2 Local spin fluctuations - Spin waves

As was seen in the previous section, the star of $\mathbf{Q}$ may consist of one or two elements in the J_1-J_2 Heisenberg model on the square lattice and the system can therefore be described by different ground state spin configurations, depending on which situation is the relevant case. The stability of these spin configurations can be investigated by allowing spin-waves, using a classical theory in terms of local spin fluctuations in the system. The Hamiltonian of the system is

$$H = \frac{1}{2}\sum_{ij} J_{ij}\mathbf{S}_i \cdot \mathbf{S}_j \tag{3.12}$$

and since there are two solutions for $\mathbf{S}_{i,j}$ the two cases will be treated separately with regards to the introduction of local spin fluctuations.

3.2.1 One element in star of Q

As was seen in Sec. (3.1.1) the star of $\mathbf{Q}$ consists of one element (either $\mathbf{Q} = (0, 0)$ or $\mathbf{Q} = \frac{1}{a}(\pi, \pi)$) when $J_2 < \frac{1}{2}|J_1|$. In this case the ground state spin configuration is given by

$$\frac{\mathbf{S}_i}{S} = \cos(\varphi_i)\hat{\boldsymbol{u}} + \sin(\varphi_j)\hat{\boldsymbol{v}}\,, \tag{3.13}$$

where $\varphi_i = \mathbf{Q} \cdot \mathbf{r}_i$. The behavior of the system when subjected to spin fluctuations will now be investigated. The existence of spin fluctuations means that the spins may deviate from the spin configuration given by Eq. (3.13), and the spin configuration of this excited state can then be described by a new $\mathbf{S}_i$

$$\mathbf{S}_i = \mathbf{S}_i^0 + \delta\mathbf{S}_i \tag{3.14}$$

where $\mathbf{S}_i^0$ are the unperturbed spins of the ground state given by Eq. (3.13) and $\delta\mathbf{S}_i$ are the deviations. These deviations can be classified by some component in two transverse directions of $\mathbf{S}_i^0$, so locally at each lattice site i

$$\mathbf{S}_i = S_i^0 \left(\cos(\varphi_i)\hat{\boldsymbol{u}} + \sin(\varphi_i)\hat{\boldsymbol{v}}\right) + S_i^1 \left(-\sin(\varphi_i)\hat{\boldsymbol{u}} + \cos(\varphi_i)\hat{\boldsymbol{v}}\right) + S_i^2 \left(\hat{\boldsymbol{u}} \times \hat{\boldsymbol{v}}\right) \tag{3.15}$$

where S_i^1 and S_i^2 then characterizes the magnitude of the deviations of the spin in each of the two transverse directions. Thus no fluctuations present locally at site i is equivalent to $(S_i^0, S_i^1, S_i^2) = (1, 0, 0)$. In terms of this spin configuration the Hamiltonian in Eq. (3.12) can be written as

$$H = \frac{1}{2}\sum_{ij} J_{ij}\left[\left(S_i^0 S_j^0 + S_i^1 S_j^1\right)\cos\left(\varphi_i - \varphi_j\right) + \left(S_i^0 S_j^1 - S_i^1 S_j^0\right)\sin\left(\varphi_i - \varphi_j\right) + S_i^2 S_j^2\right] \tag{3.16}$$

using standard trigonometric relations. Fluctuations must preserve the normalization of the spins, so $S^2 = \left(S^0\right)^2 + \left(S^1\right)^2 + \left(S^2\right)^2$. π-fields can be introduced to parametrize the fluctuations $\frac{S^\beta}{S} = \pi_\beta$ for $\beta \in \{0, 1, 2\}$. The general form of a fluctuation vector is then

$$S\left(\sqrt{1 - \pi_1^2 - \pi_2^2}, \pi_1, \pi_2\right) \simeq S\left(1 - \frac{1}{2}\left(\pi_1^2 + \pi_2^2\right), \pi_1, \pi_2\right). \tag{3.17}$$

Eq. (3.17) is valid for small fluctuations $\pi_1, \pi_2 \ll 1$. Using this assumption the Hamiltonian can be written as

$$\begin{aligned} H \simeq \frac{1}{2}S^2 \sum_{ij} J_{ij}\Bigg[&\left(1 - \frac{\pi_{1i}^2 + \pi_{2i}^2 + \pi_{1j}^2 + \pi_{2j}^2}{2} + \pi_{1i}\pi_{1j}\right)\cos(\varphi_i - \varphi_j) \\ &+ (\pi_{1j} - \pi_{1i})\sin(\varphi_i - \varphi_j) + \pi_{2i}\pi_{2j}\Bigg] \end{aligned} \tag{3.18}$$

to second order in the fluctuations. By relabeling of indices $i \to j$ and $j \to i$ the Hamiltonian can be simplified to

$$H \simeq \frac{1}{2}S^2 \sum_{ij} J_{ij}\left[\left(1 - \pi_{1i}^2 - \pi_{2i}^2 + \pi_{1i}\pi_{1j}\right)\cos\left(\varphi_i - \varphi_j\right) + 2\pi_{1i}\sin\left(\varphi_i - \varphi_j\right) + \pi_{2i}\pi_{2j}\right] \tag{3.19}$$

utilizing the fact that the exchange interaction is symmetric $J_{ji} = J_{ij}$. Inserting the Fourier transform of the π's, $\pi_{1,2i} = \frac{1}{\sqrt{\mathcal{V}}}\sum_{\mathbf{q}} \mathrm{e}^{i\mathbf{q}\cdot\mathbf{r}_i}\pi_{1,2\mathbf{q}}$ and of the exchange constant, given by Eq. (2.9), in the Hamiltonian yields

$$\begin{aligned} H = \frac{S^2}{2\mathcal{V}^2}\sum_{ij}\sum_{\mathbf{q}\mathbf{q}'\mathbf{q}''} J_{\mathbf{q}}\mathrm{e}^{i\mathbf{q}\cdot(\mathbf{r}_i-\mathbf{r}_j)}\Bigg\{\Big[\delta_{\mathbf{q},\mathbf{q}'}\delta_{\mathbf{q},\mathbf{q}''} - \pi_{1\mathbf{q}'}\pi_{1\mathbf{q}''}\mathrm{e}^{i(\mathbf{q}'+\mathbf{q}'')\cdot\mathbf{r}_i} - \pi_{2\mathbf{q}'}\pi_{2\mathbf{q}''}\mathrm{e}^{i(\mathbf{q}'+\mathbf{q}'')\cdot\mathbf{r}_i} \\ + \pi_{1\mathbf{q}'}\pi_{1\mathbf{q}''}\mathrm{e}^{i\mathbf{q}'\cdot\mathbf{r}_i+i\mathbf{q}''\cdot\mathbf{r}_j}\Big]\frac{1}{2}\left(\mathrm{e}^{i\mathbf{Q}\cdot(\mathbf{r}_i-\mathbf{r}_j)} + \mathrm{e}^{-i\mathbf{Q}\cdot(\mathbf{r}_i-\mathbf{r}_j)}\right) \\ + \frac{\sqrt{\mathcal{V}}}{i}\pi_{1\mathbf{q}'}\mathrm{e}^{i\mathbf{q}'\cdot\mathbf{r}_i}\left(\mathrm{e}^{i\mathbf{Q}\cdot(\mathbf{r}_i-\mathbf{r}_j)} - \mathrm{e}^{-i\mathbf{Q}\cdot(\mathbf{r}_i-\mathbf{r}_j)}\right) + \pi_{2\mathbf{q}'}\pi_{2\mathbf{q}''}\mathrm{e}^{i\mathbf{q}'\cdot\mathbf{r}_i+i\mathbf{q}''\cdot\mathbf{r}_j}\Bigg\} \\ = \frac{S^2}{2}J_{\mathbf{Q}} + \frac{1}{2}S^2\sum_{\mathbf{q}}\left[\left(\frac{1}{2}\left(J_{\mathbf{Q}+\mathbf{q}} + J_{\mathbf{Q}-\mathbf{q}}\right) - J_{\mathbf{Q}}\right)|\pi_{1\mathbf{q}}|^2 + \left(J_{\mathbf{q}} - J_{\mathbf{Q}}\right)|\pi_{2\mathbf{q}}|^2\right] \end{aligned} \tag{3.20}$$

where $\varphi_i - \varphi_j = \mathbf{Q}\cdot(\mathbf{r}_i - \mathbf{r}_j)$ has been employed. Identifying $|\pi_{1\mathbf{q}}|$ and $|\pi_{2\mathbf{q}}|$ as two separate modes and simplifying the spin normalization to $S = 1$, the Hamiltonian may be written neatly as

$$H = E_0 + \sum_{\mathbf{q}}\left(\omega_{1\mathbf{q}}|\pi_{1\mathbf{q}}|^2 + \omega_{2\mathbf{q}}|\pi_{2\mathbf{q}}|^2\right) \tag{3.21}$$

where

$$E_0 = \frac{1}{2}J_{\mathbf{Q}} \tag{3.22}$$

and

$$\omega_{1\mathbf{q}} = \frac{1}{4}\left(J_{\mathbf{Q}+\mathbf{q}} + J_{\mathbf{Q}-\mathbf{q}}\right) - \frac{1}{2}J_{\mathbf{Q}} \tag{3.23}$$

$$\omega_{2\mathbf{q}} = \frac{1}{2}\left(J_{\mathbf{q}} - J_{\mathbf{Q}}\right). \tag{3.24}$$

3.2.2 Two elements in star of Q

The star of $\mathbf{Q}$ consists of two elements when $J_2 > \frac{1}{2}|J_1|$, namely $\mathbf{Q}^{(1)} = \frac{1}{a}(0,\pi)$ and $\mathbf{Q}^{(2)} = \frac{1}{a}(\pi,0)$. In this case it was shown in Sec. (3.1.1) that the ground state spin configuration is

$$\mathbf{S}_i = \cos\left(\varphi_i^{(1)}\right)\cos(\Theta)\hat{\boldsymbol{u}} + \cos\left(\varphi_i^{(2)}\right)\sin(\Theta)\hat{\boldsymbol{v}} \tag{3.25}$$

where $\varphi_i^{(1)} = \mathbf{Q}^{(1)}\cdot\mathbf{r}_i$ and $\varphi_i^{(2)} = \mathbf{Q}^{(2)}\cdot\mathbf{r}_i$. As was done in the previous section, spin fluctuations can now be introduced by allowing deviations of the ground state spin configuration $\mathbf{S}_i = \mathbf{S}_i^0 + \delta\mathbf{S}_i$, and $\mathbf{S}_i^0$ is the ground state spin configuration in Eq. (3.25).

In terms of the spin components in the transverse directions of $\mathbf{S}_i^0$ the spin vectors are locally

$$\begin{aligned}\mathbf{S}_i = S_i^0 \left(\cos\left(\varphi_i^{(1)}\right)\cos(\Theta)\hat{\boldsymbol{u}} + \cos\left(\varphi_i^{(2)}\right)\sin(\Theta)\hat{\boldsymbol{v}}\right) \\ + S_i^1 \left(-\cos\left(\varphi_i^{(2)}\right)\sin(\Theta)\hat{\boldsymbol{u}} + \cos\left(\varphi_i^{(1)}\right)\cos(\Theta)\hat{\boldsymbol{v}}\right) + S_i^2\left(\hat{\boldsymbol{u}}\times\hat{\boldsymbol{v}}\right) .\end{aligned} \tag{3.26}$$

In terms of this locally fluctuating spin configuration the Hamiltonian can be written as

$$\begin{aligned}H = \frac{1}{2}\sum_{ij} J_{ij}\Big[\left(S_i^0 S_j^0 + S_i^1 S_j^1\right)\left(\cos\left(\varphi_i^{(1)}\right)\cos\left(\varphi_j^{(1)}\right)\cos^2(\Theta) + \cos\left(\varphi_i^{(2)}\right)\cos\left(\varphi_j^{(2)}\right)\sin^2(\Theta)\right) \\ + \left(S_i^0 S_j^1 - S_i^1 S_j^0\right)\left(\cos\left(\varphi_i^{(2)}\right)\cos\left(\varphi_j^{(1)}\right) - \cos\left(\varphi_i^{(1)}\right)\cos\left(\varphi_j^{(2)}\right)\right)\cos(\Theta)\sin(\Theta) + S_i^2 S_j^2\Big] .\end{aligned} \tag{3.27}$$

Utilizing relabeling of indices and the symmetry of the exchange interaction the Hamiltonian can be simplified to

$$\begin{aligned}H = \frac{1}{2}\sum_{ij} J_{ij}\Big[\left(S_i^0 S_j^0 + S_i^1 S_j^1\right)\left(\cos\left(\varphi_i^{(1)}\right)\cos\left(\varphi_j^{(1)}\right)\cos^2(\Theta) + \cos\left(\varphi_i^{(2)}\right)\cos\left(\varphi_j^{(2)}\right)\sin^2(\Theta)\right) \\ + 2\left(S_i^0 S_j^1 - S_i^1 S_j^0\right)\cos\left(\varphi_i^{(2)}\right)\cos\left(\varphi_j^{(1)}\right)\cos(\Theta)\sin(\Theta) + S_i^2 S_j^2\Big] .\end{aligned} \tag{3.28}$$

Note that $\cos\left(\varphi_i^{(1),(2)}\right)\cos\left(\varphi_j^{(1),(2)}\right) = \frac{1}{2}\left(\cos\left(\varphi_i^{(1),(2)} - \varphi_j^{(1),(2)}\right) + \cos\left(\varphi_i^{(1),(2)} + \varphi_j^{(1),(2)}\right)\right)$. Recall from Eq. (3.8) that $\mathbf{r}_i = an_i\hat{\boldsymbol{y}} + am_i\hat{\boldsymbol{z}}$ for $n_i, m_i \in \mathbb{Z}$. For $\mathbf{Q}^{(1)} = \left(0, \frac{\pi}{a}\right)$ it can be seen that $\varphi_i^{(1)} + \varphi_j^{(1)} = \mathbf{Q}^{(1)}\cdot\left(\mathbf{r}_i + \mathbf{r}_j\right) = \left(m_i + m_j\right)\pi$. Taking the cosine of this will therefore yield either $+1$ or -1 depending on if the summation $m_i + m_j$ yields an even or an odd number. However when the sum yields an even (odd) number the difference $m_i - m_j$ correspondingly yields an even (odd) number. Therefore

$$\cos\left(\varphi_i^{(1)} - \varphi_j^{(1)}\right) + \cos\left(\varphi_i^{(1)} + \varphi_j^{(1)}\right) = 2\cos\left(\varphi_i^{(1)} - \varphi_j^{(1)}\right) . \tag{3.29}$$

The same is true for any combination of (1) and (2) in $\cos\left(\varphi_i^{(1),(2)} + \varphi_j^{(1),(2)}\right)$. Thus the Hamiltonian can be simplified to

$$\begin{aligned}H = \frac{1}{2}\sum_{ij} J_{ij}\Big[\left(S_i^0 S_j^0 + S_i^1 S_j^1\right)\left(\cos\left(\varphi_i^{(1)} - \varphi_j^{(1)}\right)\cos^2(\Theta) + \cos\left(\varphi_i^{(2)} - \varphi_j^{(2)}\right)\sin^2(\Theta)\right) \\ + \left(S_i^0 S_j^1 - S_i^1 S_j^0\right)\cos\left(\varphi_i^{(2)} - \varphi_j^{(1)}\right)\sin(2\Theta) + S_i^2 S_j^2\Big]\end{aligned} \tag{3.30}$$

using $\cos(x)\sin(x) = \frac{1}{2}\sin(2x)$. Just as in the previous section, spin vectors can now be parametrized by small fluctuations $\pi_1, \pi_2 \ll 1$ preserving the normalization

$$\left(S^0, S^1, S^2\right) \simeq \left(1 - \frac{1}{2}\left(\pi_1^2 + \pi_2^2\right), \pi_1, \pi_2\right) . \tag{3.31}$$

In terms of these the Hamiltonian becomes

$$H = \frac{1}{2}\sum_{ij} J_{ij}\Big[\left(1 - \pi_{1i}^2 - \pi_{2i}^2 + \pi_{1i}\pi_{1j}\right)\left(\cos\left(\varphi_i^{(1)} - \varphi_j^{(1)}\right)\cos^2(\Theta) + \cos\left(\varphi_i^{(2)} - \varphi_j^{(2)}\right)\sin^2(\Theta)\right) + (\pi_{1j} - \pi_{1i})\cos\left(\varphi_i^{(2)} - \varphi_j^{(1)}\right)\sin(2\Theta) + \pi_{2i}\pi_{2j}\Big]. \tag{3.32}$$

Inserting the Fourier transforms of the π-fields yields a Hamiltonian in reciprocal space given by

$$\begin{aligned} H = \frac{1}{2\mathcal{V}^2}\sum_{ij}\sum_{\mathbf{q}\mathbf{q}'\mathbf{q}''} J_{\mathbf{q}} \mathrm{e}^{i\mathbf{q}\cdot(\mathbf{r}_i - \mathbf{r}_j)} \Bigg\{ \Big[\delta_{\mathbf{q},\mathbf{q}'}\delta_{\mathbf{q},\mathbf{q}''} - \pi_{1\mathbf{q}'}\pi_{1\mathbf{q}''}\mathrm{e}^{i(\mathbf{q}'+\mathbf{q}'')\cdot\mathbf{r}_i} - \pi_{2\mathbf{q}'}\pi_{2\mathbf{q}''}\mathrm{e}^{i(\mathbf{q}'+\mathbf{q}'')\cdot\mathbf{r}_i} \\ + \pi_{1\mathbf{q}'}\pi_{1\mathbf{q}''}\mathrm{e}^{i\mathbf{q}'\cdot\mathbf{r}_i + i\mathbf{q}''\cdot\mathbf{r}_j}\Big]\Big[\frac{1}{2}\left(\mathrm{e}^{i\mathbf{Q}^{(1)}\cdot(\mathbf{r}_i-\mathbf{r}_j)} + \mathrm{e}^{-i\mathbf{Q}^{(1)}\cdot(\mathbf{r}_i-\mathbf{r}_j)}\right)\cos^2(\Theta) \\ + \frac{1}{2}\left(\mathrm{e}^{i\mathbf{Q}^{(2)}\cdot(\mathbf{r}_i-\mathbf{r}_j)} + \mathrm{e}^{-i\mathbf{Q}^{(2)}\cdot(\mathbf{r}_i-\mathbf{r}_j)}\right)\sin^2(\Theta)\Big] + \pi_{2\mathbf{q}'}\pi_{2\mathbf{q}''}\mathrm{e}^{i\mathbf{q}'\cdot\mathbf{r}_i + i\mathbf{q}''\cdot\mathbf{r}_j} \\ + \frac{\sqrt{\mathcal{V}}\delta_{\mathbf{q}',\mathbf{q}''}}{2}\left(\pi_{1\mathbf{q}''}\mathrm{e}^{i\mathbf{q}''\cdot\mathbf{r}_j} - \pi_{1\mathbf{q}''}\mathrm{e}^{i\mathbf{q}''\cdot\mathbf{r}_i}\right)\left(\mathrm{e}^{i\mathbf{Q}^{(2)}\cdot\mathbf{r}_i - i\mathbf{Q}^{(1)}\cdot\mathbf{r}_j} + \mathrm{e}^{-i\mathbf{Q}^{(2)}\cdot\mathbf{r}_i + i\mathbf{Q}^{(1)}\cdot\mathbf{r}_j}\right)\sin(2\Theta)\Bigg\}. \end{aligned} \tag{3.33}$$

Carrying out the i, j sums yields

$$\begin{aligned} H = \frac{1}{2}\left(J_{\mathbf{Q}^{(1)}}\cos^2(\Theta) + J_{\mathbf{Q}^{(2)}}\sin^2(\Theta)\right) + \frac{1}{2}\sum_{\mathbf{q}}\Bigg\{\Bigg[\left(\frac{1}{2}\left(J_{\mathbf{Q}^{(1)}+\mathbf{q}} + J_{\mathbf{Q}^{(1)}-\mathbf{q}}\right) - J_{\mathbf{Q}^{(1)}}\right)\cos^2(\Theta) \\ + \left(\frac{1}{2}\left(J_{\mathbf{Q}^{(2)}+\mathbf{q}} + J_{\mathbf{Q}^{(2)}-\mathbf{q}}\right) - J_{\mathbf{Q}^{(2)}}\right)\sin^2(\Theta)\Bigg]|\pi_{1\mathbf{q}}|^2 \\ + \left(J_{\mathbf{q}} - J_{\mathbf{Q}^{(1)}}\cos^2(\Theta) - J_{\mathbf{Q}^{(2)}}\sin^2(\Theta)\right)|\pi_{2\mathbf{q}}|^2\Bigg\}. \end{aligned} \tag{3.34}$$

It is not immediately obvious why the terms linear in the π-fields vanish. They turn out to give

$$\begin{aligned} &\frac{\sin(2\Theta)}{4\mathcal{V}^{\frac{3}{2}}}\sum_{ij}\sum_{\mathbf{q}\mathbf{q}'} J_{\mathbf{q}}\mathrm{e}^{i\mathbf{q}\cdot(\mathbf{r}_i-\mathbf{r}_j)}\left(\pi_{1\mathbf{q}'}\mathrm{e}^{i\mathbf{q}'\cdot\mathbf{r}_j} - \pi_{1\mathbf{q}'}\mathrm{e}^{i\mathbf{q}'\cdot\mathbf{r}_i}\right)\left(\mathrm{e}^{i\mathbf{Q}^{(2)}\cdot\mathbf{r}_i - i\mathbf{Q}^{(1)}\cdot\mathbf{r}_j} + \mathrm{e}^{-i\mathbf{Q}^{(2)}\cdot\mathbf{r}_i + i\mathbf{Q}^{(1)}\cdot\mathbf{r}_j}\right) \\ &= \frac{1}{2}\sqrt{\mathcal{V}}\sin(2\Theta)\left(J_{\mathbf{Q}^{(2)}} - J_{\mathbf{Q}^{(1)}}\right)\left(\pi_{1\mathbf{Q}^{(1)}-\mathbf{Q}^{(2)}} + \pi_{1\mathbf{Q}^{(2)}-\mathbf{Q}^{(1)}}\right) \\ &= 0 \end{aligned} \tag{3.35}$$

since $J_{\mathbf{Q}^{(1)}} = J_{\mathbf{Q}^{(2)}} = -4J_2$, as can be seen from Eq. (3.10). So once again the Hamiltonian in Eq. (3.34) is of the form

$$H = E_0 + \sum_{\mathbf{q}} \left(\omega_{1\mathbf{q}}(\Theta) |\pi_{1\mathbf{q}}|^2 + \omega_{2\mathbf{q}}(\Theta) |\pi_{2\mathbf{q}}|^2 \right) \tag{3.36}$$

where

$$\begin{aligned} \omega_{1\mathbf{q}}(\Theta) = & \frac{1}{2} \left(\frac{1}{2} \left(J_{\mathbf{Q}^{(1)}+\mathbf{q}} + J_{\mathbf{Q}^{(1)}-\mathbf{q}} \right) - J_{\mathbf{Q}^{(1)}} \right) \cos^2(\Theta) \\ & + \frac{1}{2} \left(\frac{1}{2} \left(J_{\mathbf{Q}^{(2)}+\mathbf{q}} + J_{\mathbf{Q}^{(2)}-\mathbf{q}} \right) - J_{\mathbf{Q}^{(2)}} \right) \sin^2(\Theta) \end{aligned} \tag{3.37}$$

$$\omega_{2\mathbf{q}}(\Theta) = \frac{1}{2} \left(J_{\mathbf{q}} - J_{\mathbf{Q}^{(1)}} \cos^2(\Theta) - J_{\mathbf{Q}^{(2)}} \sin^2(\Theta) \right) \tag{3.38}$$

and

$$E_0 = \frac{1}{2} \left(J_{\mathbf{Q}^{(1)}} \cos^2(\Theta) + J_{\mathbf{Q}^{(2)}} \sin^2(\Theta) \right) . \tag{3.39}$$

3.2.3 Quantization of fluctuations

Having identified two modes in the Hamiltonian the π-fields may now be quantized in order to obtain the spin-wave dispersion relation. The fields can be quantized according to [18]

$$\left[\frac{S_x}{S}, \frac{S_y}{S} \right] = i \frac{S_z}{S^2} \tag{3.40}$$

in the large spin limit $S \to \infty$ (which can be thought of as the classical limit of the quantum mechanical case) in accordance with the canonical commutation relations. Using this, the identification $x_{\mathbf{q}} = \sqrt{2}\pi_{1\mathbf{q}}$ and $p_{\mathbf{q}} = \sqrt{2}\pi_{2\mathbf{q}}$ (which obeys $[x_{\mathbf{q}}, p_{\mathbf{q}'}] = ih\delta_{\mathbf{q},\mathbf{q}'}$) can be made. The Hamiltonian can then be written as

$$H = E_0 + \sum_{\mathbf{q}} \left(\frac{1}{2} \omega_{1\mathbf{q}} x_{-\mathbf{q}} x_{\mathbf{q}} + \frac{1}{2} \omega_{2\mathbf{q}} p_{-\mathbf{q}} p_{\mathbf{q}} \right) , \tag{3.41}$$

where E_0 depends on the ground state spin configuration (e.g. Eq. (3.22) or Eq. (3.39)). Then the second quantized spin-wave operators can be introduced

$$a_{\mathbf{q}} = \frac{1}{\sqrt{2}} \left(\frac{1}{c_{\mathbf{q}}} x_{\mathbf{q}} + \frac{i}{\hbar} c_{\mathbf{q}} p_{\mathbf{q}} \right) , \qquad a^\dagger_{-\mathbf{q}} = \frac{1}{\sqrt{2}} \left(\frac{1}{c_{\mathbf{q}}} x_{\mathbf{q}} - \frac{i}{\hbar} c_{\mathbf{q}} p_{\mathbf{q}} \right) \tag{3.42}$$

where $c_{\mathbf{q}} = \sqrt{\frac{\hbar\sqrt{\omega_{2\mathbf{q}}}}{\sqrt{\omega_{1\mathbf{q}}}}}$ and with reverse transformation

$$x_{\mathbf{q}} = \frac{c_{\mathbf{q}}}{\sqrt{2}} \left(a^\dagger_{-\mathbf{q}} + a_{\mathbf{q}} \right) , \qquad p_{\mathbf{q}} = i \frac{h}{\sqrt{2} c_{\mathbf{q}}} \left(a^\dagger_{-\mathbf{q}} - a_{\mathbf{q}} \right) . \tag{3.43}$$

In terms of these operators the Hamiltonian can then be written as

$$H = E_0 + \sum_{\mathbf{q}} \hbar\Omega_{\mathbf{q}} \left(a^\dagger_{\mathbf{q}} a_{\mathbf{q}} + \frac{1}{2} \right) \tag{3.44}$$

where

$$\Omega_{\mathbf{q}} = \sqrt{\omega_{1\mathbf{q}}\omega_{2\mathbf{q}}} \tag{3.45}$$

is the spin-wave dispersion.

One element in star of Q

In the case of one element in the star of $\mathbf{Q}$, where the spin configuration is given by Eq. (3.13), the two branches were shown to be

$$\omega_{1\mathbf{q}} = \frac{1}{4}\left(J_{\mathbf{Q}+\mathbf{q}} + J_{\mathbf{Q}-\mathbf{q}}\right) - \frac{1}{2}J_{\mathbf{Q}} \tag{3.46}$$

$$\omega_{2\mathbf{q}} = \frac{1}{2}\left(J_{\mathbf{q}} - J_{\mathbf{Q}}\right) . \tag{3.47}$$

In the J_1-J_2 Heisenberg model on the square lattice the $\mathbf{q}$-vector which minimizes the energy is given by

$$\mathbf{Q} = (Q_y, Q_z) = \begin{cases} (0,0) & \text{for } J_1 < 0,\ J_2 < \frac{1}{2}|J_1|, \\ \frac{1}{a}(\pi,\pi) & \text{for } J_1 > 0,\ J_2 < \frac{1}{2}|J_1|. \end{cases} \tag{3.48}$$

as was seen in Sec. (3.1.1). Denoting $\xi_x = \cos(xa)$, the exchange interaction from Eq. (3.10), with $a_y = a_z = a$, can be written as

$$J_{\mathbf{q}} = 2J_1\left(\xi_{q_y} + \xi_{q_z}\right) + 4J_2\xi_{q_y}\xi_{q_z} . \tag{3.49}$$

In the case of $\mathbf{Q} = (0,0)$ the spin-wave spectrum in Eq. (3.45) is quite simple since $J_{\mathbf{Q}} = 4(J_1 + J_2)$ and $J_{\mathbf{Q}\pm\mathbf{q}} = J_{\mathbf{q}}$. It is

$$\Omega_{\mathbf{q}} = \frac{1}{2}\left(J_{\mathbf{q}} - J_{\mathbf{Q}}\right) = J_1\left(\xi_{q_y} + \xi_{q_z} - 2\right) + 2J_2\left(\xi_{q_y}\xi_{q_z} - 1\right) . \tag{3.50}$$

A plot of this spin-wave dispersion can be seen in Fig. (3.4a) for $J_1 = -1$ and $J_2 = 0.1$.

When $\mathbf{Q} = \frac{1}{a}(\pi,\pi)$ the minimized exchange coupling is $J_{\mathbf{Q}} = 4(-J_1 + J_2)$ and $J_{\mathbf{Q}\pm\mathbf{q}} = -2J_1\left(\xi_{q_y} + \xi_{q_z}\right) + 4J_2\xi_{q_y}\xi_{q_z}$. Then the spin-wave spectrum given by Eq. (3.45) is

$$\Omega_{\mathbf{q}} = \sqrt{\left(J_1\left(-\xi_{q_y} - \xi_{q_z} + 2\right) + 2J_2\left(\xi_{q_y}\xi_{q_z} - 1\right)\right)\left(J_1\left(\xi_{q_y} + \xi_{q_z} + 2\right) + 2J_2\left(\xi_{q_y}\xi_{q_z} - 1\right)\right)} . \tag{3.51}$$

This spin-wave dispersion can be seen in Fig. (3.4b) for $J_1 = 1$ and $J_2 = 0.1$.

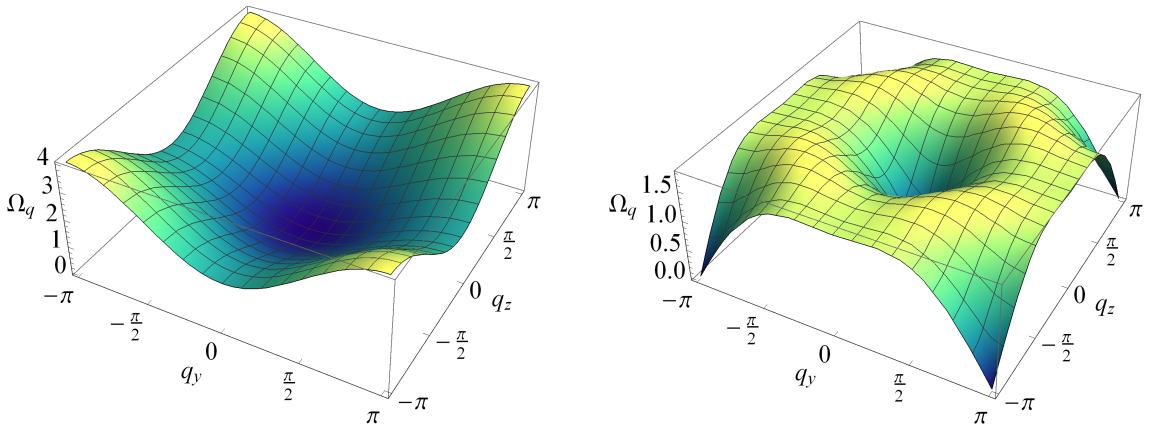

(a) $\Omega_{\mathbf{q}}$ from Eq. (3.50) for $J_1 = -1$ and $J_2 = 0.1$ where $\mathbf{Q} = (0, 0)$.

(b) $\Omega_{\mathbf{q}}$ from Eq. (3.51) for $J_1 = 1$ and $J_2 = 0.1$ where $\mathbf{Q} = \frac{1}{a}(\pi, \pi)$.

Figure 3.4: Plot of spin-wave dispersion $\Omega_{\mathbf{q}}$ for different strenghts of the Heisenberg exchange interactions J_{ij} between nearest neighboring sites (J_1) and next-nearest neighboring sites (J_2) in the two-dimensional square lattice with $a = 1$ described by the Hamiltonian given in Eq. (2.3).

Two elements in star of Q

When there are two $\mathbf{q}$-vectors in the star of $\mathbf{Q}$ for the two-dimensional square lattice, and when $2\mathbf{Q}$ is a reciprocal lattice vector for both of these $\mathbf{Q}$'s, the spin configuration is given by Eq. (3.25). Once again two branches emerge with spectra

$$\begin{aligned}\omega_{1\mathbf{q}} = &\frac{1}{2}\left(\frac{1}{2}\left(J_{\mathbf{Q}^{(1)}+\mathbf{q}} + J_{\mathbf{Q}^{(1)}-\mathbf{q}}\right) - J_{\mathbf{Q}^{(1)}}\right)\cos^2(\Theta) \\ &+ \frac{1}{2}\left(\frac{1}{2}\left(J_{\mathbf{Q}^{(2)}+\mathbf{q}} + J_{\mathbf{Q}^{(2)}-\mathbf{q}}\right) - J_{\mathbf{Q}^{(2)}}\right)\sin^2(\Theta) \qquad (3.52)\\ \omega_{2\mathbf{q}} = &\frac{1}{2}\left(J_{\mathbf{q}} - J_{\mathbf{Q}^{(1)}}\cos^2(\Theta) - J_{\mathbf{Q}^{(2)}}\sin^2(\Theta)\right) \qquad (3.53)\end{aligned}$$

and $J_{\mathbf{q}}$ is still given by (3.10). The two $\mathbf{q}$-vectors in the star of $\mathbf{Q}$ are $\mathbf{Q}^{(1)} = \left(0, \frac{\pi}{a}\right)$ and $\mathbf{Q}^{(2)} = \left(\frac{\pi}{a}, 0\right)$. Once again denoting $\xi_x = \cos(xa)$ it can be seen that

$$\begin{aligned}J_{\mathbf{Q}^{(1)}} &= J_{\mathbf{Q}^{(2)}} = -4J_2 \qquad (3.54)\\ J_{\mathbf{Q}^{(1)}\pm\mathbf{q}} &= 2J_1\left(\xi_{q_y} - \xi_{q_z}\right) - 4J_2\xi_{q_y}\xi_{q_z} \qquad (3.55)\\ J_{\mathbf{Q}^{(2)}\pm\mathbf{q}} &= 2J_1\left(-\xi_{q_y} + \xi_{q_z}\right) - 4J_2\xi_{q_y}\xi_{q_z}\,. \qquad (3.56)\end{aligned}$$

The spin-wave spectrum in Eq. (3.45) is then

$$\Omega_{\mathbf{q}} = \sqrt{J_1\left(\xi_{q_y} - \xi_{q_z}\right)\left(\cos^2(\Theta) - \sin^2(\Theta)\right) + 2J_2\left(1 - \xi_{q_y}\xi_{q_z}\right)} \sqrt{J_1\left(\xi_{q_y} + \xi_{q_z}\right) + 2J_2\left(1 + \xi_{q_y}\xi_{q_z}\right)}\,. \qquad (3.57)$$

This spin-wave dispersion can be seen in Fig. (3.5) for different angles Θ. In general an angle of $\Theta + \frac{\pi}{2}$ rotates the figure by $\frac{\pi}{2}$ compared to that of angle Θ.

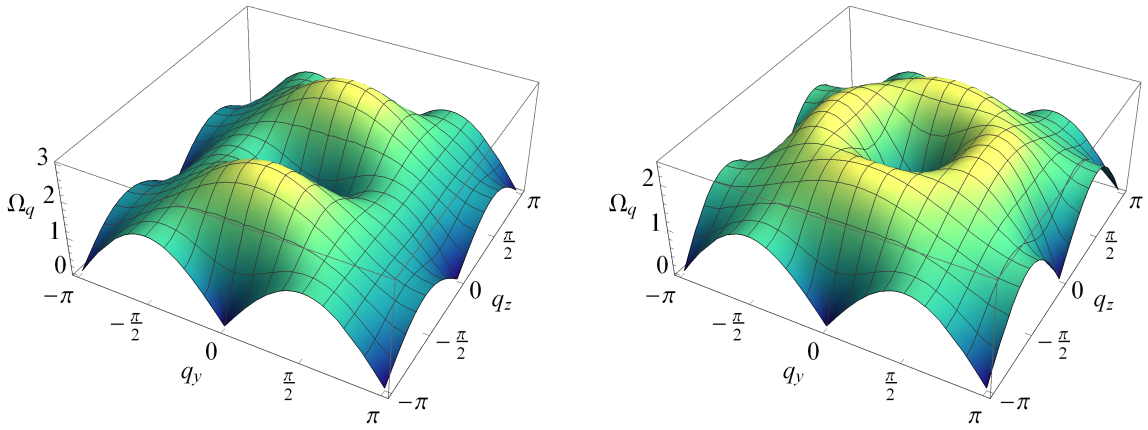

(a) $\Omega_{\mathbf{q}}$ for $J_1 = J_2 = 1$, $\Theta = 0$.

(b) $\Omega_{\mathbf{q}}$ for $J_1 = J_2 = 1$, $\Theta = \frac{\pi}{4}$.

Figure 3.5: Plot of spin-wave dispersion $\Omega_{\mathbf{q}}$ from Eq. (3.57) for different angles Θ, where $2\Theta = \theta$ is the angle between spins of the two antiferromagnetic sublattices of the ground state spin configuration, see Fig. (3.6) in the two-dimensional square lattice with $a = 1$.

3.3 Quantum spin fluctuations - Magnons

So far the spin-wave dispersion has been obtained using a classical spin-wave theory while treating the spin operators as classical vectors, which were then quantized. However the spin operators are inherently quantum mechanical objects, and a suitable quantum mechanical approach to determine the spin-wave dispersion will now be applied. A Holstein-Primakoff transformation of the spin operators will be employed to obtain a bilinear Hamiltonian, to which a Bogoliubov transformation then can readily be applied.

3.3.1 Holstein-Primakoff transformation

The Holstein-Primakoff transformation describes the relation between the spin projection operators and the magnon creation and annihilation operators in second quantization [19]. The transformation is given by [20]

$$S_i^+ = S_i^x + iS_i^y = \sqrt{2S - b_i^\dagger b_i} b_i \tag{3.58}$$

$$S_i^- = S_i^x - iS_i^y = b_i^\dagger \sqrt{2S - b_i^\dagger b_i} \tag{3.59}$$

$$S_i^z = S - b_i^\dagger b_i \,. \tag{3.60}$$

The operators in Eqs. (3.58)-(3.60) satisfy the necessary commutation relation for the spin operator projections $\left[S^\alpha, S^\beta\right] = \epsilon_{\alpha\beta\gamma} i S^\gamma$, where $\alpha, \beta \in \{x, y, z\}$. $b_i^\dagger$ and b_i are the bosonic magnon creation and annihilation operators and they obey the bosonic commutation relations

$$[b_i, b_j] = 0\,, \qquad \left[b_i^\dagger, b_j^\dagger\right] = 0\,, \qquad \left[b_i, b_j^\dagger\right] = \delta_{i,j}\,. \tag{3.61}$$

In the limit of large spin S (compared to the magnon creation and annihilation operators) the spin operators can be expanded in powers of $\frac{1}{S}$ yielding

$$S_i^+ \simeq \sqrt{2S} b_i \tag{3.62}$$
$$S_i^- \simeq \sqrt{2S} b_i^\dagger \tag{3.63}$$
$$S_i^z = S - b_i^\dagger b_i \,. \tag{3.64}$$

In the J_1-J_2 Heisenberg model for $J_2 > \frac{1}{2}|J_1|$ the ground state spin configuration of the two-dimensioanal square lattice consists of two antiferromagnetic sublattices, differing by a relative angle θ, as discussed in Sec. (3.1.1), see Fig. (3.1). The Hamiltonian describing the system is given by Eq. (2.3). The Holstein-Primakoff representations are defined in local coordinate systems, in which the spins are parallel to the local z-axis. To be able to apply this method a rotation by angle θ_i of each spin $\mathbf{S}_i$ in the lattice is done, so that is becomes parallel with the z-axis. Using the rotation matrix

$$R_x(\phi) = \begin{pmatrix} 1 & 0 & 0 \\ 0 & \cos(\phi) & -\sin(\phi) \\ 0 & \sin(\phi) & \cos(\phi) \end{pmatrix} \tag{3.65}$$

which describes a rotation by angle ϕ around the x-axis, which is the only rotation relevant here, since all spins lie in the yz-plane, whereas for a three-dimensional system two rotation matrices would be necessary. For the rotation matrices it is evident that $R_x^{-1}(\phi) = R_x(-\phi)$ and $R_x(\phi_a)R_x(\phi_b) = R_x(\phi_a + \phi_b)$, which is true for rotations about any axis, not just the x-axis. Additionally the rotation matrices are orthogonal matrices, such that $R_x^{\mathrm{T}} R_x = R_x^{-1} R_x = \mathbb{1}$. The Hamiltonian can therefore be written as

$$\begin{aligned} H &= \frac{1}{2}\sum_{ij} J_{ij} \mathbf{S}_i \cdot \mathbf{S}_j \\ &= \frac{1}{2}\sum_{ij} J_{ij} \mathbf{S}_i R_x^{-1}(\theta_i) R_x(\theta_i) \cdot R_x^{-1}(\theta_j) R_x(\theta_j) \mathbf{S}_j \\ &= \frac{1}{2}\sum_{ij} J_{ij} \tilde{\mathbf{S}}_i R_x(\theta_i - \theta_j) \tilde{\mathbf{S}}_j \end{aligned} \tag{3.66}$$

where $\tilde{\mathbf{S}}_{i,j} = R_x(\theta_{i,j})\mathbf{S}_{i,j}$ are the spin operators defined in the local reference frame. These rotated spin operators still obey the required commutation relation $\left[\tilde{S}^\alpha, \tilde{S}^\beta\right] = \epsilon_{\alpha\beta\gamma} i \tilde{S}^\gamma$. Because of the form of R_x, given by Eq. (3.65), the Hamiltonian can be simplified to

$$H = \frac{1}{2}\sum_{ij} J_{ij} \left[\tilde{S}_i^x \tilde{S}_j^x + \cos(\theta_i - \theta_j)\left(\tilde{S}_i^y \tilde{S}_j^y + \tilde{S}_i^z \tilde{S}_j^z\right) + \sin(\theta_i - \theta_j)\left(\tilde{S}_i^z \tilde{S}_j^y - \tilde{S}_i^y \tilde{S}_j^z\right)\right] . \tag{3.67}$$

Noting that $S_i^x = \frac{1}{2}\left(S_i^+ + S_i^-\right)$ and $S_i^y = \frac{1}{2i}\left(S_i^+ - S_i^-\right)$ the Hamiltonian becomes

$$H \simeq \frac{S}{2}\sum_{ij} J_{ij}\Bigg\{\frac{1+\cos(\theta_i-\theta_j)}{2}\left(b_i^\dagger b_j + b_i b_j^\dagger\right) + \frac{1-\cos(\theta_i-\theta_j)}{2}\left(b_i^\dagger b_j^\dagger + b_i b_j\right)$$
$$-\cos(\theta_i-\theta_j)\left(b_i^\dagger b_i + b_j^\dagger b_j\right) + S\cos(\theta_i-\theta_j) + \sin(\theta_i-\theta_j)\, i\sqrt{\frac{S}{2}}\left(b_i^\dagger - b_j^\dagger - b_i + b_j\right)\Bigg\} \tag{3.68}$$

to second order in the Holstein-Primakoff bosons in the large S expansion, given by Eqs. (3.62)-(3.64). Using the trigonometric identities $\frac{1}{2}(1+\cos(x)) = \cos^2\left(\frac{x}{2}\right)$ and $\frac{1}{2}(1-\cos(x)) = \sin^2\left(\frac{x}{2}\right)$ the Hamiltonian can be written as

$$H \simeq \frac{S}{2}\sum_{ij} J_{ij}\Bigg\{\cos^2\left(\frac{\theta_i-\theta_j}{2}\right)\left(b_i^\dagger b_j + b_i b_j^\dagger\right) + \sin^2\left(\frac{\theta_i-\theta_j}{2}\right)\left(b_i^\dagger b_j^\dagger + b_i b_j\right)$$
$$-\cos(\theta_i-\theta_j)\left(b_i^\dagger b_i + b_j^\dagger b_j\right) + S\cos(\theta_i-\theta_j) + \sin(\theta_i-\theta_j)\, i\sqrt{\frac{S}{2}}\left(b_i^\dagger - b_j^\dagger - b_i + b_j\right)\Bigg\}. \tag{3.69}$$

This Hamiltonian can be simplified by utilizing relabelling of indeces $i \to j$ and $j \to i$ and keeping in mind that the exchange constant is symmetric $J_{ji} = J_{ij}$, as is cosine $\cos(\theta_j-\theta_i) = \cos(\theta_i-\theta_j)$ while sine is asymmetric $\sin(\theta_j-\theta_i) = -\sin(\theta_i-\theta_j)$. The full Hamiltonian describing the J_1-J_2 Heisenberg model using the Holstein-Primakoff representation is then

$$H \simeq \frac{S}{2}\sum_{ij} J_{ij}\Bigg\{2\cos^2\left(\frac{\theta_i-\theta_j}{2}\right) b_i^\dagger b_j + \sin^2\left(\frac{\theta_i-\theta_j}{2}\right)\left(b_i^\dagger b_j^\dagger + b_i b_j\right) - 2\cos(\theta_i-\theta_j)\, b_i^\dagger b_i$$
$$+ S\cos(\theta_i-\theta_j) + 2\sin(\theta_i-\theta_j)\, i\sqrt{\frac{S}{2}}\left(b_i^\dagger - b_i\right)\Bigg\}. \tag{3.70}$$

Next the Fourier transform of the Holstein-Primakoff bosons will be inserted

$$b_i = \frac{1}{\sqrt{\mathcal{V}}}\sum_{\mathbf{q}} \mathrm{e}^{i\mathbf{q}\cdot\mathbf{r}_i} b_{\mathbf{q}} \tag{3.71}$$

$$b_i^\dagger = \frac{1}{\sqrt{\mathcal{V}}}\sum_{\mathbf{q}} \mathrm{e}^{-i\mathbf{q}\cdot\mathbf{r}_i} b_{\mathbf{q}}^\dagger \tag{3.72}$$

and the contributions from the nearest and the next-nearest neighbors will be determined separately. As it is very important to be careful in the following derivation, since there are lots of traps to fall in, the derivation will be done in full for each term in the Hamiltonian.

Nearest neighbor contribution

The ground state spin configuration of the J_1-J_2 Heisenberg model consists of two different types of spin vectors, along with the antiferromagnetic partner of each of these, so four different vectors in total, see Fig. (3.6).

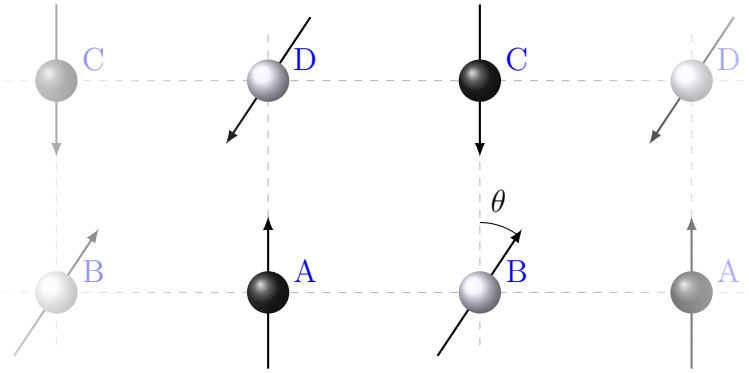

Figure 3.6: Spin configuration in ground state of J_1-J_2 Heisenberg model with the four possible different types of spin vectors A, B, C and D.

A spin at site i is coupled to their 4 nearest neighbors by exchange constant $J_{ij} = J_1$, see Fig. (3.1). The difference in the angle with the z-axis between spins A and C have with their nearest neighboring sites are

$$\theta_{A,C} - \theta_j = \begin{cases} -\theta & \text{for nearest neighbors in the } y\text{-direction,} \\ -\theta \pm \pi & \text{for nearest neighbors in the } z\text{-direction} \end{cases} \tag{3.73}$$

and for spins B and D

$$\theta_{B,D} - \theta_j = \begin{cases} \theta & \text{for nearest neighbors in the } y\text{-direction,} \\ \theta \pm \pi & \text{for nearest neighbors in the } z\text{-direction.} \end{cases} \tag{3.74}$$

Employing this the terms of the J_1-J_2 Heisenberg Hamltonian in Eq. (3.70) can be determined in $\mathbf{q}$-space upon insertion of the Fourier transform of the bosonic creation and annihilation operators. Firstly consider

$$\begin{aligned} S\sum_{\langle ij\rangle} J_{ij}\cos^2\left(\frac{\theta_i-\theta_j}{2}\right) b_i^\dagger b_j &= \frac{S}{\mathcal{V}} J_1 \sum_{\langle ij\rangle}\sum_{\mathbf{q}\mathbf{q}'} \cos^2\left(\frac{\theta_i-\theta_j}{2}\right) \mathrm{e}^{-i\mathbf{q}\cdot\mathbf{r}_i}\mathrm{e}^{i\mathbf{q}'\cdot\mathbf{r}_j} b_{\mathbf{q}}^\dagger b_{\mathbf{q}'} \\ &= \frac{S}{\mathcal{V}} J_1 \sum_{i\mathbf{q}\mathbf{q}'} \mathrm{e}^{-i(\mathbf{q}-\mathbf{q}')\cdot\mathbf{r}_i}\left(\cos^2\left(\frac{\theta}{2}\right)\left[\mathrm{e}^{iq_y'a}+\mathrm{e}^{-iq_y'a}\right] + \sin^2\left(\frac{\theta}{2}\right)\left[\mathrm{e}^{iq_z'a}+\mathrm{e}^{-iq_z'a}\right]\right) b_{\mathbf{q}}^\dagger b_{\mathbf{q}'} \\ &= 2SJ_1 \sum_{\mathbf{q}}\left[\cos^2\left(\frac{\theta}{2}\right)\cos\left(q_y a\right) + \sin^2\left(\frac{\theta}{2}\right)\cos\left(q_z a\right)\right] b_{\mathbf{q}}^\dagger b_{\mathbf{q}} \end{aligned} \tag{3.75}$$

where $\sum\langle ij\rangle$ denotes a sum over nearest neighbor sites only and noting that $\cos^2\left(\frac{\pm\theta\pm\pi}{2}\right) = \sin^2\left(\frac{\theta}{2}\right)$. Using

$$\sum_{\mathbf{q}} b_{\mathbf{q}}^\dagger b_{\mathbf{q}} = \sum_{-\mathbf{q}} b_{-\mathbf{q}}^\dagger b_{-\mathbf{q}} \tag{3.76}$$

this can be rewritten to

$$\begin{aligned} &2SJ_1 \sum_{\mathbf{q}} \left[\cos^2\left(\frac{\theta}{2}\right) \cos\left(q_y a\right) + \sin^2\left(\frac{\theta}{2}\right) \cos\left(q_z a\right) \right] b^\dagger_{\mathbf{q}} b_{\mathbf{q}} \\ &= SJ_1 \sum_{\mathbf{q}} \left[\cos^2\left(\frac{\theta}{2}\right) \cos\left(q_y a\right) + \sin^2\left(\frac{\theta}{2}\right) \cos\left(q_z a\right) \right] \left(b^\dagger_{\mathbf{q}} b_{\mathbf{q}} + b^\dagger_{-\mathbf{q}} b_{-\mathbf{q}} \right) . \end{aligned} \tag{3.77}$$

Similarly

$$\begin{aligned} &\frac{S}{2} \sum_{\langle ij \rangle} J_{ij} \sin^2\left(\frac{\theta_i - \theta_j}{2}\right) \left(b^\dagger_i b^\dagger_j + b_i b_j \right) \\ &= \frac{S}{2\mathcal{V}} J_1 \sum_{\langle ij \rangle} \sum_{\mathbf{q}\mathbf{q}'} \sin^2\left(\frac{\theta_i - \theta_j}{2}\right) \left(\mathrm{e}^{-i\mathbf{q}\cdot\mathbf{r}_i} \mathrm{e}^{-i\mathbf{q}'\cdot\mathbf{r}_j} b^\dagger_{\mathbf{q}} b^\dagger_{\mathbf{q}'} + \mathrm{e}^{i\mathbf{q}\cdot\mathbf{r}_i} \mathrm{e}^{i\mathbf{q}'\cdot\mathbf{r}_j} b_{\mathbf{q}} b_{\mathbf{q}'} \right) \\ &= SJ_1 \sum_{\mathbf{q}} \left[\sin^2\left(\frac{\theta}{2}\right) \cos\left(q_y a\right) + \cos^2\left(\frac{\theta}{2}\right) \cos\left(q_z a\right) \right] \left(b^\dagger_{\mathbf{q}} b^\dagger_{-\mathbf{q}} + b_{\mathbf{q}} b_{-\mathbf{q}} \right) \end{aligned} \tag{3.78}$$

and

$$\begin{aligned} -S \sum_{\langle ij \rangle} J_{ij} \cos\left(\theta_i - \theta_j\right) b^\dagger_i b_i &= -\frac{SJ_1}{\mathcal{V}} \sum_{\langle ij \rangle} \sum_{\mathbf{q}\mathbf{q}'} \cos\left(\theta_i - \theta_j\right) \mathrm{e}^{-i(\mathbf{q}-\mathbf{q}')\cdot\mathbf{r}_i} b^\dagger_{\mathbf{q}} b_{\mathbf{q}'} \\ &= -\frac{SJ_1}{\mathcal{V}} \sum_{i} \sum_{\mathbf{q}\mathbf{q}'} i \mathrm{e}^{-i(\mathbf{q}-\mathbf{q}')\cdot\mathbf{r}_i} b^\dagger_{\mathbf{q}} b_{\mathbf{q}'} \left[2\cos(\theta) - 2\cos(\theta) \right] \\ &= 0 . \end{aligned} \tag{3.79}$$

Lastly consider one of the terms linear in the magnon operators

$$\begin{aligned} \sum_{\langle ij \rangle} J_{ij} \sin(\theta_i - \theta_j) b^\dagger_i &= \frac{J_1}{\sqrt{\mathcal{V}}} \sum_{\langle ij \rangle} \sum_{\mathbf{q}} \sin(\theta_i - \theta_j) \mathrm{e}^{-i\mathbf{q}\cdot\mathbf{r}_i} b^\dagger_{\mathbf{q}} \\ &= \frac{J_1}{\sqrt{\mathcal{V}}} \sum_{i\mathbf{q}} \mathrm{e}^{-i\mathbf{q}\cdot\mathbf{r}_i} \left[2\sin(\theta) - 2\sin(\theta) \right] b^\dagger_{\mathbf{q}} \\ &= 0 . \end{aligned} \tag{3.80}$$

All similar linear terms vanish in the same manner. In a similar approach the remaining constant term is

$$\frac{S^2}{2} \sum_{\langle ij \rangle} J_{ij} \cos\left(\theta_i - \theta_j\right) = \frac{S^2}{2} J_1 \sum_{i} \left[2\cos(\theta) - 2\cos(\theta) \right] = 0 . \tag{3.81}$$

All contributions from nearest neighboring site interacions have now been determined, and the next-nearest neighbor contribution will be established.

Next-nearest neighbor contribution

A site and their next-nearest neighbor is coupled by exchange constant $J_{ij} = J_2$, see Fig. (3.1). Because of the nature of the ground state consisting of two antiferromagnetic sublattices, the difference in angle between a site and their next-nearest neighbors is

$$\theta_i - \theta_j = \pm\pi \tag{3.82}$$

for i any of the four spins A, B, C or D in Fig. (3.6). From this, it is immediately apparent that terms in the Hamiltonian given by Eq. (3.70) with $\cos^2\left(\frac{\theta_i-\theta_j}{2}\right)$ and $\sin(\theta_i - \theta_j)$ vanish. First consider

$$\begin{aligned}
&\frac{S}{2}\sum_{\langle\langle ij\rangle\rangle} J_{ij}\sin^2\left(\frac{\theta_i-\theta_j}{2}\right)\left(b_i^\dagger b_j^\dagger + b_i b_j\right) = \frac{SJ_2}{2\mathcal{V}}\sum_{\langle\langle ij\rangle\rangle}\sum_{\mathbf{q}\mathbf{q}'}\left(\mathrm{e}^{-i\mathbf{q}\cdot\mathbf{r}_i}\mathrm{e}^{-i\mathbf{q}'\cdot\mathbf{r}_j} b_{\mathbf{q}}^\dagger b_{\mathbf{q}'}^\dagger + \mathrm{e}^{i\mathbf{q}\cdot\mathbf{r}_i}\mathrm{e}^{i\mathbf{q}'\cdot\mathbf{r}_j} b_{\mathbf{q}} b_{\mathbf{q}'}\right) \\
&= \frac{SJ_2}{2\mathcal{V}}\sum_{i\mathbf{q}\mathbf{q}'}\Bigg[\mathrm{e}^{-i(\mathbf{q}+\mathbf{q}')\cdot\mathbf{r}_i}\left(\mathrm{e}^{i\left(q_y'a+q_z'a\right)} + \mathrm{e}^{i\left(q_y'a-q_z'a\right)} + \mathrm{e}^{i\left(-q_y'a+q_z'a\right)} + \mathrm{e}^{-i\left(q_y'a+q_z'a\right)}\right) b_{\mathbf{q}}^\dagger b_{\mathbf{q}'}^\dagger \\
&+ \mathrm{e}^{i(\mathbf{q}+\mathbf{q}')\cdot\mathbf{r}_i}\left(\mathrm{e}^{i\left(q_y'a+q_z'a\right)} + \mathrm{e}^{i\left(q_y'a-q_z'a\right)} + \mathrm{e}^{i\left(-q_y'a+q_z'a\right)} + \mathrm{e}^{-i\left(q_y'a+q_z'a\right)}\right) b_{\mathbf{q}} b_{\mathbf{q}'}\Bigg] \\
&= 2SJ_2\sum_{\mathbf{q}}\cos\left(q_y a\right)\cos\left(q_z a\right)\left(b_{\mathbf{q}}^\dagger b_{-\mathbf{q}}^\dagger + b_{\mathbf{q}} b_{-\mathbf{q}}\right)
\end{aligned} \tag{3.83}$$

where $\sum_{\langle\langle ij\rangle\rangle}$ denotes a sum over next-nearest neighbors. Secondly consider

$$\begin{aligned}
-S\sum_{\langle\langle ij\rangle\rangle} J_{ij}\cos\left(\theta_i-\theta_j\right) b_i^\dagger b_i &= \frac{4SJ_2}{\mathcal{V}}\sum_{i\mathbf{q}\mathbf{q}'}\mathrm{e}^{-i(\mathbf{q}-\mathbf{q}')\cdot\mathbf{r}_i} b_{\mathbf{q}}^\dagger b_{\mathbf{q}'} \\
&= 4SJ_2\sum_{\mathbf{q}} b_{\mathbf{q}}^\dagger b_{\mathbf{q}} \\
&= 2SJ_2\sum_{\mathbf{q}}\left(b_{\mathbf{q}}^\dagger b_{\mathbf{q}} + b_{-\mathbf{q}}^\dagger b_{-\mathbf{q}}\right) .
\end{aligned} \tag{3.84}$$

Lastly the constant term is

$$\frac{S^2}{2}\sum_{\langle\langle ij\rangle\rangle} J_{ij}\cos\left(\theta_i-\theta_j\right) = -2S^2 J_2 N\,. \tag{3.85}$$

Having calculated all contributions the bosonic Bogoliubov transformation can now be employed to determine the spin-wave spectrum.

3.3.2 Bosonic Bogoliubov transformation

Collecting the contributions from the nearest and next-nearest neighbors the Hamiltonian in Eq. (3.70) can be written on a bilinear form

$$H = \mathcal{C} + \sum_{\mathbf{q}} \left[\mathcal{E}_0 \left(b^\dagger_{\mathbf{q}} b_{\mathbf{q}} + b^\dagger_{-\mathbf{q}} b_{-\mathbf{q}} \right) + \mathcal{E}_1 \left(b^\dagger_{\mathbf{q}} b^\dagger_{-\mathbf{q}} + b_{\mathbf{q}} b_{-\mathbf{q}} \right) \right] \tag{3.86}$$

where

$$\mathcal{C} = -2S^2 J_2 N \tag{3.87}$$

$$\frac{\mathcal{E}_0}{S} = J_1 \cos^2\left(\frac{\theta}{2}\right) \cos\left(q_y a\right) + J_1 \sin^2\left(\frac{\theta}{2}\right) \cos\left(q_z a\right) + 2J_2 \tag{3.88}$$

$$\frac{\mathcal{E}_1}{S} = J_1 \sin^2\left(\frac{\theta}{2}\right) \cos\left(q_y a\right) + J_1 \cos^2\left(\frac{\theta}{2}\right) \cos\left(q_z a\right) + 2J_2 \cos(q_y a) \cos(q_z a) \tag{3.89}$$

in the J_1-J_2 Heisenberg model on a two-dimensional lattice. To diagonalize the Hamiltonian in Eq. (3.86) a bosonic Bogoliubov transformation may be applied. This transformation converts the Hamiltonian to a diagonal form by performing a linear transformation of the bosonic operators

$$b_{\mathbf{q}} = u\alpha_{\mathbf{q}} - v\beta^\dagger_{\mathbf{q}} \tag{3.90}$$

$$b_{-\mathbf{q}} = u\beta_{\mathbf{q}} - v\alpha^\dagger_{\mathbf{q}} \tag{3.91}$$

where α and β are also bosonic operators obeying the bosonic commutation relations, which can easily be verified. When doing so it is evident that $u^2 - v^2 = 1$. Inserting the Bogoliubov transformation in the Hamiltonian in Eq. (3.86) it becomes

$$H = \mathcal{C} + \sum_{\mathbf{q}} \Omega_{\mathbf{q}} \left(\alpha^\dagger_{\mathbf{q}} \alpha_{\mathbf{q}} + \beta^\dagger_{\mathbf{q}} \beta_{\mathbf{q}} + 1 \right) \tag{3.92}$$

and the diagonalization has been achieved. By parametrizing $u = \cosh(t)$ and $v = \sinh(t)$ the eigenvalues can be rewritten to

$$\Omega_{\mathbf{q}} = \left(u^2 + v^2\right) \mathcal{E}_0 - 2uv\mathcal{E}_1 = \sqrt{\mathcal{E}_0^2 - \mathcal{E}_1^2}\,. \tag{3.93}$$

Inserting the expressions from Eq. (3.88) and Eq. (3.89) the spin-wave spectrum becomes

$$\begin{aligned} \Omega_{\mathbf{q}} = \Big[& \left(J_1 \left(\xi_{q_y} \cos^2(\Theta) + \xi_{q_z} \sin^2(\Theta) \right) + 2J_2 \right)^2 \\ & - \left(J_1 \left(\xi_{q_y} \sin^2(\Theta) + \xi_{q_z} \cos^2(\Theta) \right) + 2J_2 \xi_{q_y} \xi_{q_z} \right)^2 \Big]^{\frac{1}{2}} \\ & = \sqrt{J_1 \left(\xi_{q_y} - \xi_{q_z} \right) \left(\cos^2(\Theta) - \sin^2(\Theta) \right) + 2J_2 \left(1 - \xi_{q_y} \xi_{q_z} \right)} \\ & \sqrt{J_1 \left(\xi_{q_y} + \xi_{q_z} \right) + 2J_2 \left(1 + \xi_{q_y} \xi_{q_z} \right)} \end{aligned} \tag{3.94}$$

using $2\Theta = \theta$. Comparing Eq. (3.57) and Eq. (3.94) it is evident that the same spin-wave dispersion relation has been obtained using a classical and a quantum mechanical

spin-wave theory.

This dispersion relation can be used to investigate the degenerate state that occurs when $J_2 = \frac{1}{2}|J_1|$, as described in Sec. (3.1.1). In this case no unique $\mathbf{q}$-vector minimizing the energy exists, as the entire continuous edge of the Brillouin Zone may be used as $\mathbf{Q}$. No discernible spin-wave dispersion can therefore be determined, but the dispersion for $J_2 > |J_1|$ may be considered in this limit. This can be seen for different angles in Fig. (3.7).

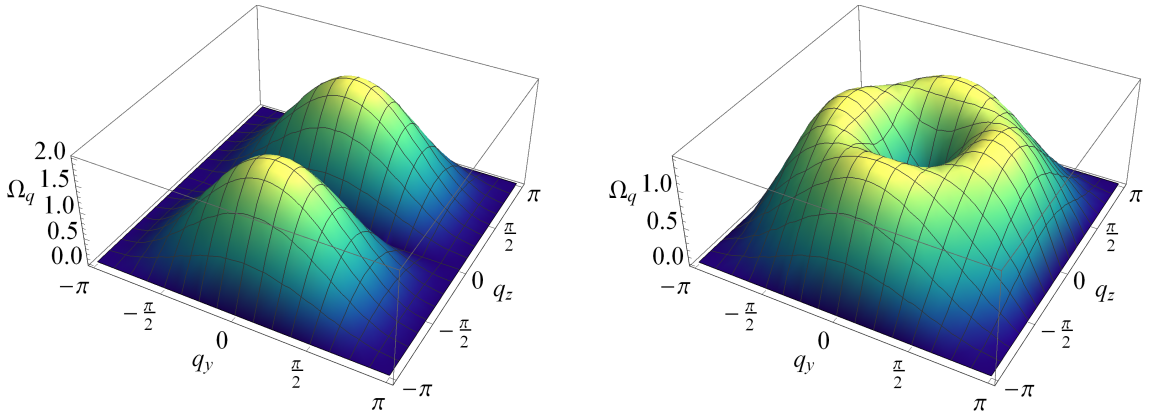

(a) $\Omega_{\mathbf{q}}$ for $\Theta = 0$.

(b) $\Omega_{\mathbf{q}}$ for $\Theta = \frac{\pi}{4}$.

Figure 3.7: Plot of spin-wave dispersion $\Omega_{\mathbf{q}}$ from Eq. (3.57) at the degenerate point $J_2 = \frac{1}{2}|J_1|$ for different angles Θ, where $2\Theta = \theta$ is the angle between spins of the two antiferromagnetic sublattices of the ground state spin configuration, see Fig. (3.6) in the two-dimensional square lattice with $a = 1$.

Ref. [21] shows that the free energy of the system is minimized for $\theta = 0, \pi$. The system is therefore ordered while subject to thermal fluctuations to a greater extent than the zero temperature ground state. The same is the case for quantum fluctuations [21]. This is an example of the phenomenon of so-called order by disorder.

Group velocities

For small $\mathbf{q}$ the spin-wave spectrum in Eq. (3.94) can be expanded to second order in $\mathbf{q}$. Considering $\Theta = 0$ this yields an approximate dispersion

$$\Omega_{\mathbf{q}} \simeq \sqrt{(J_1 + 2J_2)^2 q_y^2 + (J_1 + 2J_2)(-J_1 + 2J_2) q_z^2}\,. \tag{3.95}$$

At the highly frustrated point $J_2 = \frac{1}{2}|J_1|$, and the dispersion therefore reduces to

$$\Omega_{\mathbf{q}} \simeq \pm 2J_1 q_y \tag{3.96}$$

i.e. there is no dependency on q_z, which gives rise to the continuous spectrum of zero-energy modes. The group velocities along the y and z axes are

$$v_y = \frac{\partial \Omega_{\mathbf{q}}}{\partial q_y} = \frac{2\left(J_1 + 2J_2\right)^2}{\Omega_{\mathbf{q}}} q_y \tag{3.97}$$

$$v_z = \frac{\partial \Omega_{\mathbf{q}}}{\partial q_z} = \frac{2\left(J_1 + 2J_2\right)\left(-J_1 + 2J_2\right)}{\Omega_{\mathbf{q}}} q_z \,. \tag{3.98}$$

It is evident that the group velocities differ along the two axes. Having gone throught the J_1-J_2 Heisenberg model, additional interactions may now be added, to determine the effect that this has on the system.

Chapter 4

The orthorhombic lattice

In this chapter it is investigated how the breaking of a symmetry affects the Heisenberg model on the two-dimensional lattice described in Ch. (3). In this case it is the C_4 symmetry of the lattice which is reduced to a C_2 symmetry, by stretching the lattice, so that the lattice constants $a_y \neq a_z$, which will affect the strengths of the exchange couplings. An orthorhombic J_{1y}-J_{1z}-J_2 lattice is investigated and the spin-wave spectrum is calculated, both in a straightforward manner and by letting J_1 differ in the y and z direction at the frustrated point $J_2 = \frac{1}{2}|J_1|$ arising in the J_1-J_2 model on the two-dimensional square lattice described in Sec. (3.1.1).

4.1 Ground state spin configuration

So far the Heisenberg model has been used on the two-dimensional square lattice where the lattice constants are equal $a_y = a_z$, see Ch. (3). A system which does not fulfill this similarity of the lattice constants is the orthorhombic lattice, in which $a_y \neq a_z$, see Fig. (4.1) for an example with $a_y > a_z$.

In the orthorhombic lattice there are no longer four nearest neighbors to a site i, but only two. Once again the system is described by the Heisenberg Hamiltonian in Eq. (2.3). The two-dimensional orthorhombic lattice in the yz-plane, which can be described by the J_{1y}-J_{1z}-J_2 Heisenberg model, will be investigated. Here a site is coupled to their neighbors by an exchange constant given by

$$J_{ij} = \begin{cases} J_{1y} & \text{for an immediate neighbor } j \text{ in the } y\text{-direction,} \\ J_{1z} & \text{for an immediate neighbor } j \text{ in the } z\text{-direction,} \\ J_2 & \text{for a neighbor } j \text{ at } \mathbf{r}_i \pm a_y\hat{\boldsymbol{y}} \pm a_z\hat{\boldsymbol{z}}. \end{cases} . \tag{4.1}$$

J_2 describes the coupling to the third nearest neighbor when the lattice constants fulfill $\sqrt{a_y^2 + a_z^2} < 2a_z$ and $a_y > a_z$. One should be careful with excessive stretching of the

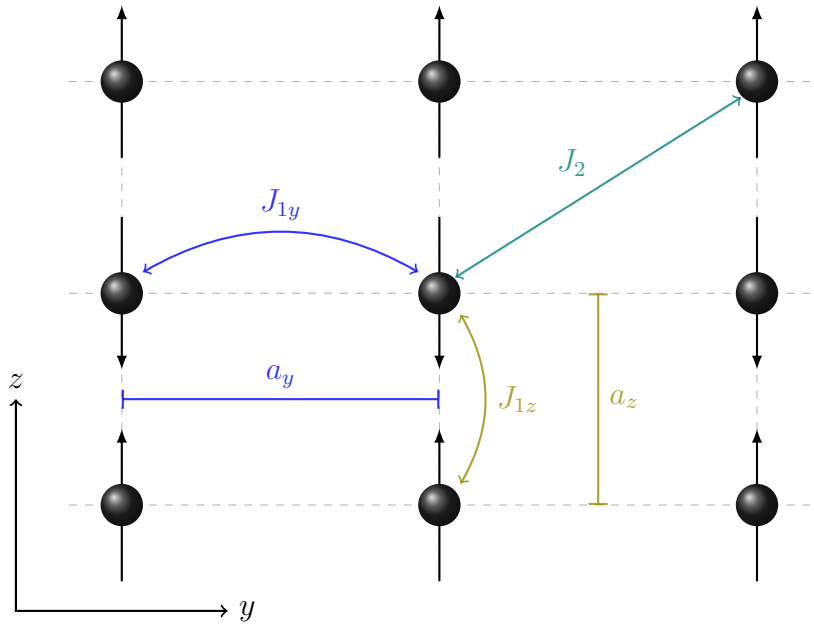

Figure 4.1: Illustration of an example of an orthorhombic spin lattice structure with different exchange constants in different directions of the lattice

lattice as this might result in the sites at $\mathbf{r}_i \pm 2a_z\hat{\boldsymbol{z}}$ being third nearest neighbors. However this only poses a problem in the description of a site coupling to its nearest, second nearest and third nearest neighbors. In that case the exchange constant in Eq. (4.1) may still be used, but the sites then actually couple to their nearest, second nearest and fourth nearest neighbors. In the following $\sqrt{a_y^2 + a_z^2} < 2a_z$ and $a_y > a_z$ will be assumed, so that Eq. (4.1) describes the coupling to the nearest, second nearest and third nearest neighbors and couplings to neighbors further away are neglected.

The Hamiltonian can be written in $\mathbf{q}$-space by inserting the Fourier transform of the spins, given by Eq. (2.7). It becomes

$$H = \frac{1}{2}\sum_{\mathbf{q}} J_{\mathbf{q}}\mathbf{S}_{\mathbf{q}} \cdot \mathbf{S}_{-\mathbf{q}} \tag{4.2}$$

where

$$J_{\mathbf{q}} = 2J_{1y}\cos\left(q_y a_y\right) + 2J_{1z}\cos(q_z a_z) + 4J_2\cos(q_y a_y)\cos(q_z a_z)\,. \tag{4.3}$$

Minimizing the energy of the system, given by Eq. (3.6), corresponds to minimizing $J_{\mathbf{q}}$ with respect to $\mathbf{q}$. As was seen in Sec. (3.1.1) the ground state spin configuration can be characterized by

$$\mathbf{S}_i = \cos\left(\mathbf{Q}\cdot\mathbf{r}_i\right)\hat{\boldsymbol{u}} + \sin\left(\mathbf{Q}\cdot\mathbf{r}_i\right)\hat{\boldsymbol{v}}\,. \tag{4.4}$$

The $\mathbf{q}$-vector which minimizes the energy, denoted $\mathbf{Q}$, depends on the interactions strengths J_{1y}, J_{1z} and J_2. $J_{\mathbf{q}}$ is plotted for different combinations of these in Fig. (4.2).

Just as in the case of the square lattice described in Sec. (3.1.1), there are two cases of interaction strengths which result in a self-evident ground state. When $J_{1y}, J_{1z}, J_2 < 0$ all exchange interactions prefer alignment of the spins, and $\mathbf{Q} = (0, 0)$ resulting in a ferromagnetic ground state spin configuration. When $J_{1y}, J_{1z} > 0$ and $J_2 < 0$ all interactions can again be satisfied simultaneously, and $\mathbf{Q} = \left(\frac{\pi}{a_y}, \frac{\pi}{a_z}\right)$ and an antiferromagnetic ground state spin configuration emerges. A contour plot of this situation can be seen in Fig. (4.2a).

Contrarily, when $J_2 > 0$ the third nearest neighbor interaction energy is minimized when the corresponding spins are antiparallel, which cannot be fulfilled simultaneously with the J_1 interactions, no matter the sign of these. This leads to a change in the value of $\mathbf{Q}$ to either $\left(0, \frac{\pi}{a_z}\right)$, see Fig. (4.2b), or $\left(\frac{\pi}{a_y}, 0\right)$, i.e. an antiferromagnetic stripe in either the y or z direction depending on the exact strengths of the exchange interactions. But the degeneracy which was seen in Sec. (3.1.1) where every point on the edge of the Brillouin Zone could be used as $\mathbf{Q}$ is no longer present, since J_1 no longer has the same contribution to the energy for neighboring sites in the y-direction and in the z-direction. Additionally the frustration arising because of the two $\mathbf{q}$-vectors ($\mathbf{Q}^{(1)} = \frac{1}{a}(0, \pi)$ and $\mathbf{Q}^{(2)} = \frac{1}{a}(\pi, 0)$) minimizing the energy in the J_1-J_2 model, when $J_2 > \frac{1}{2}|J_1|$, has also vanished in the orthorhombic lattice, as one of these will always correspond to a lower energy than the other.

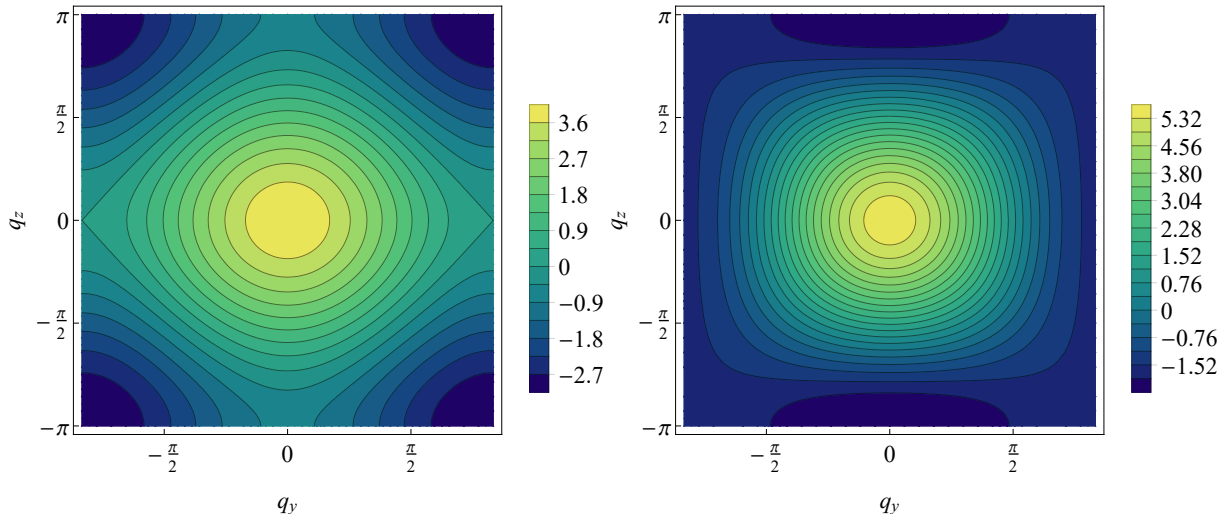

(a) $J_{\mathbf{q}}$ for $J_{1y} = 0.8$, $J_{1z} = 1$, $J_2 = 0.1$.

(b) $J_{\mathbf{q}}$ for $J_{1y} = 0.8$, $J_{1z} = 1$, $J_2 = 0.5$.

Figure 4.2: Contour plot of $J_{\mathbf{q}}$ from Eq. (4.3) for different strengths of the exchange interactions J_{1y}, J_{1z} and J_2 between sites in the two-dimensional orthorhombic lattice with $a_y = 1.2$ and $a_z = 1$. The minimum of $J_{\mathbf{q}}$ shifts from $\mathbf{Q} = \left(\frac{\pi}{a_y}, \frac{\pi}{a_z}\right)$ to $\mathbf{Q} = \left(0, \frac{\pi}{a_z}\right)$ as J_2 increases.

In Fig. (4.2) a linear relation between the lattice constant and the corresponding exchange interaction has been assumed. When the distance between two atoms decreases it is fair to assume that the interaction between them grows stronger, and likewise when the

distance increases the interaction strength must decrease. Concretely $J_{1y,z} = -a_{y,z} + 2$ has been assumed.

Since the C_4 symmetry of the square lattice has been reduced to a C_2 symmetry in the orthorhombic lattice the degeneracy of the ground state, which is apparent in Fig. (3.2) and Fig. (3.3) is broken. The competition between the J_2 and J_1's is never frustrated, and there is never more than one $\mathbf{q}$-vector which minimizes the energy. Therefore the ground state spin configuration is given by Eq. (4.4) [13].

4.2 Classical fluctuations - Spin waves

The stability of the classical ground state of the orthorhombic lattice may now be investigated by introducing spin deviations. The procedure for obtaining the spin-wave dispersion is completely analogous to that of the J_1-J_2 Heisenberg model, which was done in Sec. (3.2). The only difference is that of the exchange interactions $J_{\mathbf{q}}$, but this does not affect the derivation. Therefore the derivation will be done swiftly here. The ground state spin configuration is given by Eq. (4.4). By introducing spin deviations S_i^1 and S_i^2 in the two transverse directions of the ground state S_i^0, the spin configuration can be written as

$$\mathbf{S}_i = S_i^0 \left(\cos(\varphi_i)\hat{\boldsymbol{u}} + \sin(\varphi_i)\hat{\boldsymbol{v}}\right) + S_i^1 \left(-\sin(\varphi_i)\hat{\boldsymbol{u}} + \cos(\varphi_i)\hat{\boldsymbol{v}}\right) + S_i^2 \left(\hat{\boldsymbol{u}} \times \hat{\boldsymbol{v}}\right) . \tag{4.5}$$

Inserting this in the Hamiltonian and parameterizing the fluctuations by π-fields

$$\left(S^0, S^1, S^2\right) \simeq \left(1 - \frac{1}{2}\left(\pi_1^2 + \pi_2^2\right), \pi_1, \pi_2\right) \tag{4.6}$$

for small fluctuations $\pi_1, \pi_2 \ll 1$ yields a Hamiltonian given by

$$H = E_0 + \sum_{\mathbf{q}} \left(\omega_{1\mathbf{q}}|\pi_{1\mathbf{q}}|^2 + \omega_{2\mathbf{q}}|\pi_{2\mathbf{q}}|^2\right) \tag{4.7}$$

in $\mathbf{q}$-space, where $E_0 = \frac{1}{2}J_{\mathbf{Q}}$ and

$$\omega_{1\mathbf{q}} = \frac{1}{4}\left(J_{\mathbf{Q}+\mathbf{q}} + J_{\mathbf{Q}-\mathbf{q}}\right) - \frac{1}{2}J_{\mathbf{Q}} \tag{4.8}$$

$$\omega_{2\mathbf{q}} = \frac{1}{2}\left(J_{\mathbf{q}} - J_{\mathbf{Q}}\right) . \tag{4.9}$$

The spin fluctuations may be quantized according to the derivation in Sec. (3.2.3) and the spin-wave dispersion is then given by

$$\Omega_{\mathbf{q}} = \sqrt{\omega_{1\mathbf{q}}\omega_{2\mathbf{q}}} . \tag{4.10}$$

Denoting $\xi_{q_\alpha} = \cos(q_\alpha a_\alpha)$ the exchange interaction in Eq. (4.3) can be written as $J_{\mathbf{q}} = 2J_{1y}\xi_{q_y} + 2J_{1z}\xi_{q_z} + 4J_2\xi_{q_y}\xi_{q_z}$. For $\mathbf{Q} = (0,0)$ the minimized exchange interaction is $J_{\mathbf{Q}} = 2\left(J_{1y} + J_{1z}\right) + 4J_2$ and $J_{\mathbf{Q}\pm\mathbf{q}} = J_{\mathbf{q}}$. The spin-wave spectrum is then

$$\Omega_{\mathbf{q}} = \frac{1}{2}\left(J_{\mathbf{q}} - J_{\mathbf{Q}}\right) = J_{1y}\left(\xi_{q_y} - 1\right) + J_{1z}\left(\xi_{q_z} - 1\right) + 2J_2\left(\xi_{q_y}\xi_{q_s} - 1\right) \tag{4.11}$$

which reduces to Eq. (3.50) for $J_{1y} = J_{1z}$ as it should. For $\mathbf{Q} = \left(\frac{\pi}{a_y}, \frac{\pi}{a_z}\right)$ the minimal exchange interaction is $J_{\mathbf{Q}} = -2\left(J_{1y} + J_{1z}\right) + 4J_2$ and $J_{\mathbf{Q}\pm\mathbf{q}} = -2\left(J_{1y}\xi_{q_y} + J_{1z}\xi_{q_z}\right) + 4J_2\xi_{q_y}\xi_{q_z}$, so the spin-wave dispersion is

$$\omega_{\mathbf{q}} = \sqrt{J_{1y}\left(1 - \xi_{q_y}\right) + J_{1z}\left(1 - \xi_{q_z}\right) + 2J_2\left(\xi_{q_y}\xi_{q_z} - 1\right)} \sqrt{J_{1y}\left(\xi_{q_y} + 1\right) + J_{1z}\left(\xi_{q_z} + 1\right) + 2J_2\left(\xi_{q_y}\xi_{q_z} - 1\right)} \tag{4.12}$$

which reduces to Eq. (3.51) for $J_{1y} = J_{1z}$. As J_2 increases the minimum of $J_{\mathbf{q}}$ shifts to $\mathbf{Q} = \left(0, \frac{\pi}{a_z}\right)$ or $\mathbf{Q} = \left(\frac{\pi}{a_y}, 0\right)$, depending on the exact geometry of the orthorhombic lattice. For $\mathbf{Q} = \left(0, \frac{\pi}{a_z}\right)$, the exchange interaction is $J_{\mathbf{Q}} = 2\left(J_{1y} - J_{1z}\right) - 4J_2$ and $J_{\mathbf{Q}\pm\mathbf{q}} = 2\left(J_{1y}\xi_{q_y} - J_{1z}\xi_{q_z}\right) - 4J_2\xi_{q_y}\xi_{q_z}$ and the spin-wave spectrum is

$$\Omega_{\mathbf{q}} = \sqrt{J_{1y}\left(\xi_{q_y} - 1\right) + J_{1z}\left(1 - \xi_{q_z}\right) + 2J_2\left(1 - \xi_{q_y}\xi_{q_z}\right)} \sqrt{J_{1y}\left(\xi_{q_y} - 1\right) + J_{1z}\left(\xi_{q_z} + 1\right) + 2J_2\left(\xi_{q_y}\xi_{q_z} + 1\right)} \tag{4.13}$$

which reduces to Eq. (3.57) for $J_{1y} = J_{1z}$ and $\Theta = 0$ or $\Theta = \pi$. A plot of the spin-wave dispersion in this case is presented in Fig. (4.3a).

To see how stretching of the lattice affects the frustration of the J_1-J_2 Heisenberg model on the square lattice described in Sec. (3.2.2) this model may be investigated in the J_{1y}-J_{1z}-J_2 model. Initially assume no difference between J_{1y} and J_{1z} and two elements in the star of $\mathbf{Q}$, $\mathbf{Q}^{(1)} = \left(0, \frac{\pi}{a_z}\right)$ and $\mathbf{Q}^{(2)} = \left(\frac{\pi}{a_y}, 0\right)$. The ground state spin configuration is then given by

$$\mathbf{S}_i = \cos\left(\varphi_i^{(1)}\right)\cos(\Theta)\hat{\boldsymbol{u}} + \cos\left(\varphi_i^{(2)}\right)\sin(\Theta)\hat{\boldsymbol{v}}\,. \tag{4.14}$$

The derivation of the two modes $\omega_{1\mathbf{q}}$ and $\omega_{2\mathbf{q}}$ is done in Sec. (3.2.2) and results in

$$\omega_{1\mathbf{q}} = \frac{1}{2}\left(\frac{1}{2}\left(J_{\mathbf{Q}^{(1)}+\mathbf{q}} + J_{\mathbf{Q}^{(1)}-\mathbf{q}}\right) - J_{\mathbf{Q}^{(1)}}\right)\cos^2(\Theta) \tag{4.15}$$

$$+ \frac{1}{2}\left(\frac{1}{2}\left(J_{\mathbf{Q}^{(2)}+\mathbf{q}} + J_{\mathbf{Q}^{(2)}-\mathbf{q}}\right) - J_{\mathbf{Q}^{(2)}}\right)\sin^2(\Theta) \tag{4.16}$$

$$\omega_{2\mathbf{q}} = \frac{1}{2}\left(J_{\mathbf{q}} - J_{\mathbf{Q}^{(1)}}\cos^2(\Theta) - J_{\mathbf{Q}^{(2)}}\sin^2(\Theta)\right)\,. \tag{4.17}$$

In the J_{1y}-J_{1z}-J_2 model the spin-wave dispersion then becomes

$$\Omega_{\mathbf{q}} = \Big[\left(J_{1y} \left(\xi_{q_y} - 1 \right) + J_{1z} \left(1 - \xi_{q_z} \right) + 2J_2 \left(1 - \xi_{q_y} \xi_{q_z} \right) \right) \cos^2 \left(\Theta \right) + \left(J_{1y} \left(1 - \xi_{q_y} \right) + J_{1z} \left(\xi_{q_z} - 1 \right) + 2J_2 \left(1 - \xi_{q_y} \xi_{q_z} \right) \right) \sin^2 \left(\Theta \right) \Big]^{\frac{1}{2}} \Big[J_{1y} \left(\xi_{q_y} - \cos^2 \left(\Theta \right) + \sin^2 \left(\Theta \right) \right) + J_{1z} \left(\xi_{q_z} + \cos^2 \left(\Theta \right) - \sin^2 \left(\Theta \right) \right) + 2J_2 \left(\xi_{q_y} \xi_{q_z} + 1 \right) \Big]^{\frac{1}{2}}. \tag{4.18}$$

The dispersion in Eq. (4.18) is presented in Fig. (4.3b). Comparing this figure with Fig. (3.7a) it is evident that the lines of zero-energy modes vanishes, as the energy is raised due to $a_y \neq a_z$.

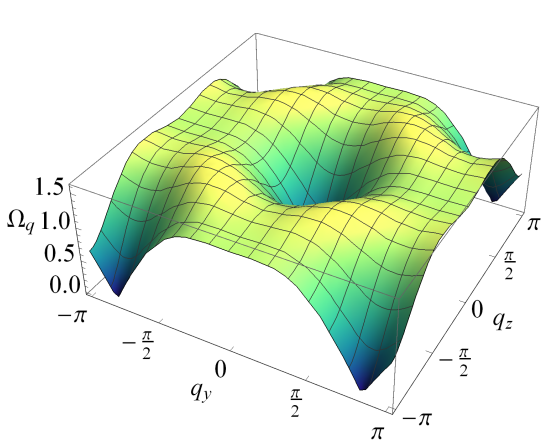

(a) $\Omega_{\mathbf{q}}$ from Eq. (4.13), for $J_{1y} = 0.8$, $J_{1z} = 1$ and $J_2 = 0.1$. $\Theta = 0$.

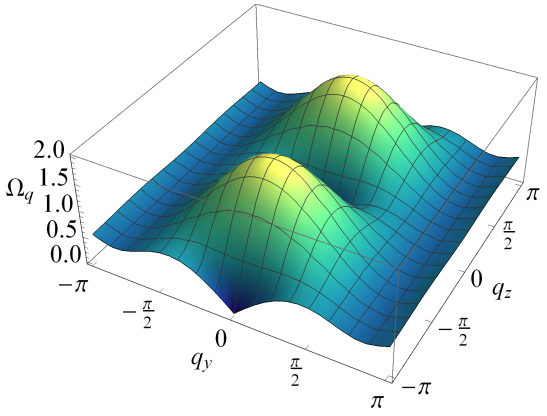

(b) $\Omega_{\mathbf{q}}$ from Eq. (4.18) for $J_{1y} = 0.8$, $J_{1z} = 1$, $J_2 = 0.5$ and

Figure 4.3: Plot of spin-wave dispersion $\Omega_{\mathbf{q}}$ for different interactions strengths in the two-dimensional orthorhombic lattice in the J_{1y}-J_{1z}-J_2 Heisenberg model.

Chapter 5

Anisotropic Dzyaloshinsky-Moriya exchange interaction

In this chapter the effect that adding the anisotropic Dzyaloshinsky-Moriya (DM) interaction to the J_1-J_2 Heisenberg model on the two-dimensional square lattice is determined. The inversion symmetry of the lattice is broken as a result of the form of the DM interaction. The ground state spin configuration is determined and thereafter subjected to spin fluctuations. A spin-wave dispersion is obtained using a classical local spin fluctuations theory and a quantum Holstein-Primakoff transformation.

5.1 Ground state spin configuration

In a system with both symmetric and antisymmetric exchange interactions, the Hamiltonian is given by

$$H = \sum_{ij} \left[\frac{1}{2} J_{ij} \mathbf{S}_i \cdot \mathbf{S}_j + \mathbf{D}_{ij} \cdot (\mathbf{S}_i \times \mathbf{S}_j) \right] . \tag{5.1}$$

To find the ground state spin configuration, the Luttinger-Tisza method is employed, based on [16]. The energy of the system is minimized under the weak constraint rather that the local constraint, as explained in Sec. (2.3)

$$0 = \frac{\partial}{\partial S_i^\alpha} \left[H - \lambda \left(\sum_i |\mathbf{S}_i|^2 - \mathcal{N} S^2 \right) \right] , \tag{5.2}$$

for $\alpha \in \{x, y, z\}$, where S_i^α is the α-component of the spin vector. This method utilizes a single Lagrange multiplier λ and gives the set of equations

$$\sum_{\mathbf{q}} \mathrm{e}^{i\mathbf{r}_i\cdot\mathbf{q}} \left(\lambda S^x_{\mathbf{q}}\right) = \sum_{\mathbf{q}} \mathrm{e}^{i\mathbf{r}_i\cdot\mathbf{q}} \left(\frac{1}{2} J_{\mathbf{q}} S^x_{\mathbf{q}} + S^y_{\mathbf{q}} D^z_{\mathbf{q}} - S^z_{\mathbf{q}} D^y_{\mathbf{q}}\right) \tag{5.3}$$

$$\sum_{\mathbf{q}} \mathrm{e}^{i\mathbf{r}_i\cdot\mathbf{q}} \left(\lambda S^y_{\mathbf{q}}\right) = \sum_{\mathbf{q}} \mathrm{e}^{i\mathbf{r}_i\cdot\mathbf{q}} \left(\frac{1}{2} J_{\mathbf{q}} S^y_{\mathbf{q}} + S^z_{\mathbf{q}} D^x_{\mathbf{q}} - S^x_{\mathbf{q}} D^z_{\mathbf{q}}\right) \tag{5.4}$$

$$\sum_{\mathbf{q}} \mathrm{e}^{i\mathbf{r}_i\cdot\mathbf{q}} \left(\lambda S^z_{\mathbf{q}}\right) = \sum_{\mathbf{q}} \mathrm{e}^{i\mathbf{r}_i\cdot\mathbf{q}} \left(\frac{1}{2} J_{\mathbf{q}} S^z_{\mathbf{q}} + S^x_{\mathbf{q}} D^y_{\mathbf{q}} - S^y_{\mathbf{q}} D^x_{\mathbf{q}}\right) \tag{5.5}$$

which can be written compactly as

$$\sum_{\mathbf{q}} \mathrm{e}^{i\mathbf{q}\cdot\mathbf{r}_i} \left(\lambda S^\alpha_{\mathbf{q}}\right) = \sum_{\mathbf{q}} \mathrm{e}^{i\mathbf{q}\cdot\mathbf{r}_i} \left(\frac{1}{2} J_{\mathbf{q}} S^\alpha_{\mathbf{q}} + \left[\mathbf{S}_{\mathbf{q}} \times \mathbf{D}_{\mathbf{q}}\right]^\alpha\right) . \tag{5.6}$$

The Fourier components in Eq. (5.6) must be equal, which leads to a set of three equations, which are then to be solved for λ. In the following section this is done for a two-dimensional square lattice.

5.1.1 J_1-J_2 Heisenberg model with DM interaction

Consider the two-dimensional square lattice with lattice points in the yz-plane. In the J_1-J_2 Heisenberg model, the exchange constant J_{ij} is present for sites coupled to their nearest neighbor, with coupling strength J_1, and for sites coupled to their next-nearest neighbor, with coupling strength J_2, as can be seen in Fig. (5.1). When the DM interaction is also present in the two-dimensional square lattice, it couples nearest neighboring sites by coupling vector $\mathbf{D}_{ij}$, which can be expressed as [22, 23]

$$\mathbf{D}_{ij} = \begin{pmatrix} -D\,\mathrm{sgn}\left(y_i - y_j\right)\delta_{z_i,z_j} \\ 0 \\ 0 \end{pmatrix} \tag{5.7}$$

where D is the interaction strength and $y_{i,j}$ and $z_{i,j}$ are the coordinates of the lattice site in the y- and z-direction, respectively.

When using the DM interaction in Eq. (5.7), the set of equations, originating from the demand that the Fourier components in Eq. (5.6) are equal, simplifies to

$$\lambda S^\alpha_{\mathbf{q}} = \frac{1}{2} J_{\mathbf{q}} S^\alpha_{\mathbf{q}} + S^z_{\mathbf{q}} D^x_{\mathbf{q}} \delta_{\alpha,y} - S^y_{\mathbf{q}} D^x_{\mathbf{q}} \delta_{\alpha,z} \,. \tag{5.8}$$

Eq. (5.8) has two solutions

1. $\lambda = \frac{1}{2} J_{\mathbf{Q}}$ and $S^{y,z}_{\mathbf{Q}} = 0$
2. $\lambda = \frac{1}{2} J_{\mathbf{Q}} \pm i D^x_{\mathbf{Q}}$ and $S^x_{\mathbf{Q}} = 0$.

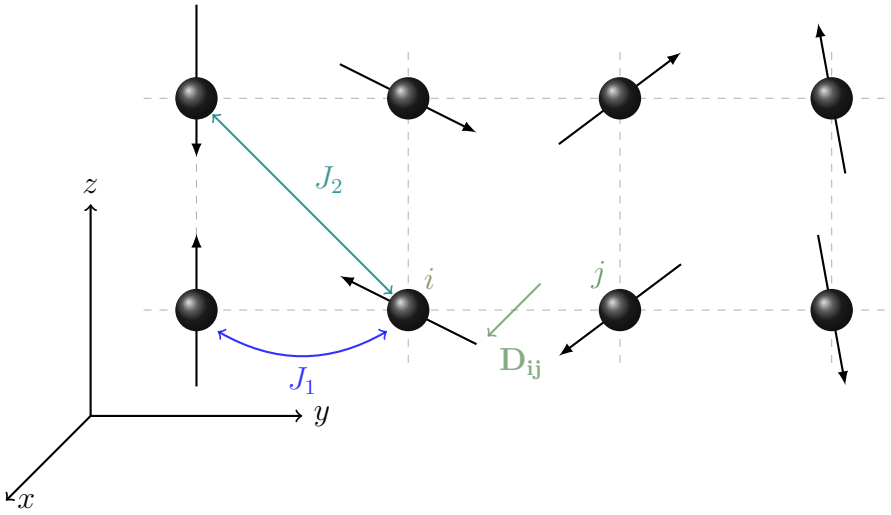

Figure 5.1: Two-dimensional square lattice with nearest (J_1) and next-nearest (J_2) neighbor Heiseneberg exchange coupling and nearest-neighbor anisotropic Dzyaloshinsky-Moriya exchange coupling $\mathbf{D}_{ij}$.

$\mathbf{Q}$ is the $\mathbf{q}$-vector which minimizes the energy. As an ansatz for the classical spins the spiral

$$S_i^\alpha = A^\alpha \cos\left(\mathbf{Q}\cdot\mathbf{r}_i + \phi^\alpha\right) \tag{5.9}$$

is used. Eq. (5.9) fulfills the eigenvalue equation in Eq. (5.8) if $A_y = A_z$, $\phi^y = \phi$ and $\phi^z = \phi + \frac{\pi}{2}$, which in turn also ensures that the local constraint is fulfilled. The spin configuration is then

$$\mathbf{S}_i = S\sin\left(\mathbf{Q}\cdot\mathbf{r}_i + \phi\right)\hat{\boldsymbol{v}} + S\cos\left(\mathbf{Q}\cdot\mathbf{r}_i + \phi\right)\hat{\boldsymbol{u}} \tag{5.10}$$

where $\hat{\boldsymbol{u}} \perp \hat{\boldsymbol{v}}$. For simplicity the phase is set to $\phi = 0$ henceforth. Inserting the Fourier transforms of the spins and the exchange interactions, given by Eq. (2.7), Eq. (2.9) and Eq. (2.11), in the Hamiltonian in Eq. (5.1) yields the Hamiltonian in reciprocal space. This is

$$H = \sum_{\mathbf{q}} \left[J_{\mathbf{q}}\mathbf{S}_{\mathbf{q}}\times\mathbf{S}_{-\mathbf{q}} + \mathbf{D}_{-\mathbf{q}}\cdot\left(\mathbf{S}_{\mathbf{q}}\times\mathbf{S}_{-\mathbf{q}}\right)\right] \tag{5.11}$$

where

$$J_{\mathbf{q}} = 2J_1\left(\cos\left(q_y a\right) + \cos\left(q_z a\right)\right) + 4J_2\cos\left(q_y a\right)\cos\left(q_z a\right) \tag{5.12}$$

$$\mathbf{D}_{\mathbf{q}} = 2iD\sin\left(q_y a\right)\hat{\boldsymbol{x}}\,. \tag{5.13}$$

The energy of the system is then

$$E = \frac{\mathcal{V}}{2}J_{\mathbf{Q}} - \frac{\mathcal{V}}{i}\mathbf{D}_{\mathbf{Q}}\cdot\hat{\boldsymbol{t}} \tag{5.14}$$

where $\hat{\boldsymbol{t}} = \hat{\boldsymbol{u}} \times \hat{\boldsymbol{v}}$. The energy is evidently minimized when $\mathbf{D_Q}$ is perpendicular to the planar spiral. In the two-dimensional square lattice $\mathbf{D_Q}$ only has a component in the x direction, which therefore forces the planar spiral to be in the yz-plane. By minimizing the energy yields $\mathbf{Q} = (Q_y, Q_z)$ as a function of the different interactions strengths, it can be seen that Q_z is always either π or 0 no matter the strengths of the other interactions. The choice of π or 0 only depends on the sign of J_1. For $J_1 > 0$ ($J_1 < 0$) $Q_z = \pi$ ($Q_z = 0$). On the other hand Q_y does depend on the interaction strenghts, and it can be expressed as $Q_y = \tan^{-1}\left(\frac{2D}{2J_2 - J_1}\right)$. A contour plot of the energy in Eq. (5.14) can be seen in Fig. (5.2). The frustration seen in the J_1-J_2 Heisenberg model in Sec. (3.1.1) is broken by the addition of the DM interaction and there is never more than one $\mathbf{q}$ in the star of $\mathbf{Q}$ when the DM interaction is present.

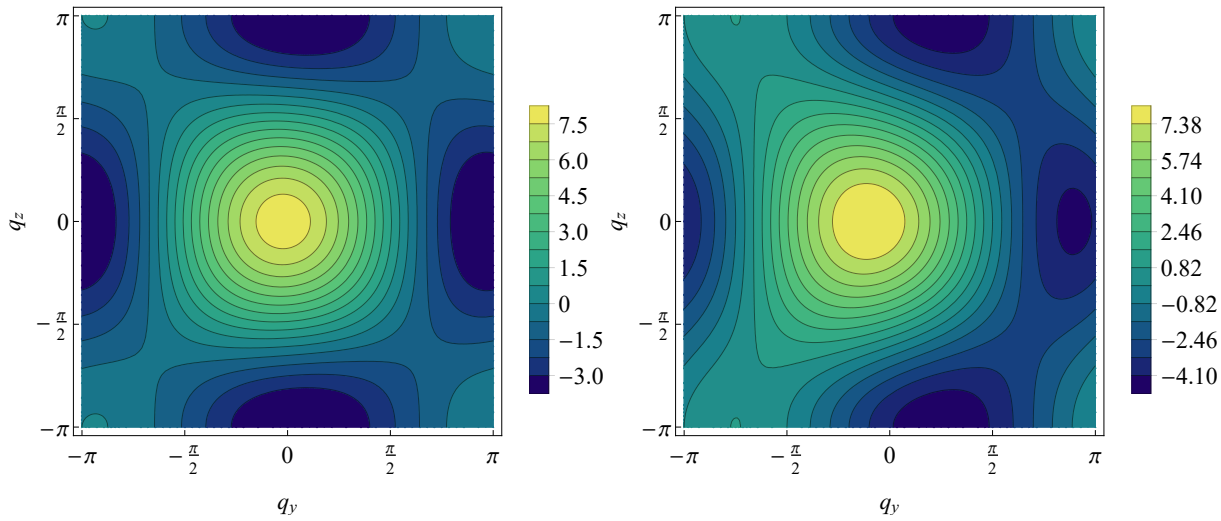

(a) E for $J_1 = 1$, $J_2 = 1$ and $D = 0.2$.

(b) E for $J_1 = 1$, $J_2 = 1$ and $D = 1$.

Figure 5.2: Contour plot of the energy E from Eq. (5.14) for different strengths of the Heisenberg exchange interactions between nearest (J_1) and next-nearest (J_2) neighboring sites and the DM interaction strength D in the two-dimensional square lattice.

5.1.2 Adding an external magnetic field

The addition of an external magnetic field, and thereby a Zeeman interaction between the magnetic field and the magnetic moments, is described by the Hamiltonian

$$H = \sum_{ij} \left[\frac{1}{2} J_{ij}\, \mathbf{S}_i \cdot \mathbf{S}_j + \mathbf{D}_{ij} \cdot (\mathbf{S}_i \times \mathbf{S}_j) \right] + g\mu_B \mathbf{B} \cdot \sum_i \mathbf{S}_i \tag{5.15}$$

where g is the g-factor and μ_B is the Bohr magneton, for a general external magnetic field $\mathbf{B} = (B^x, B^y, B^z)$. The additional term of the coupling between the B-field and the magnetic moments results in an extra term in the set of eigenvalue equations in Eq. (5.8), so that

$$\lambda S^{\alpha}_{\mathbf{q}} = \frac{1}{2} J_{\mathbf{q}} S^{\alpha}_{\mathbf{q}} + S^{z}_{\mathbf{q}} D^{x}_{\mathbf{q}} \delta_{\alpha,y} - S^{y}_{\mathbf{q}} D^{x}_{\mathbf{q}} \delta_{\alpha,z} + g\mu_B B^{\alpha} \delta_{\mathbf{q},0} \,. \tag{5.16}$$

In this case, a separate solution for $\mathbf{q} = 0$ emerges, where $\lambda \neq \frac{1}{2} J_0$ and $\mathbf{S}_0 = \frac{g\mu_B \mathbf{B}}{\lambda - \frac{1}{2} J_0}$. For $\mathbf{q} = \mathbf{Q} \neq 0$ the solutions from Sec. (5.1.1) are still valid. Using the ansatz in Eq. (5.9) and imposing the local constraint makes it evident that a homogeneous $\mathbf{q} = 0$ can only be added if it is in a direction which is perpendicular to the spiral solution, so that $\mathbf{S}_0 \perp \hat{\boldsymbol{u}}$ and $\mathbf{S}_0 \perp \hat{\boldsymbol{v}}$. This fixes the uv-plane to be perpendicular to $\mathbf{B}$. In this case the spin configuration becomes

$$\mathbf{S}_i = \beta \hat{\boldsymbol{t}} + \sqrt{1 - \beta^2} \left[\cos\left(\mathbf{Q} \cdot \mathbf{r}_i + \phi\right) \hat{\boldsymbol{u}} + \sin\left(\mathbf{Q} \cdot \mathbf{r}_i\right) \hat{\boldsymbol{v}} \right] \tag{5.17}$$

where $\beta = \frac{g\mu_B}{\lambda - \frac{1}{2} J_0} |\mathbf{B}|$ and $\lambda = \frac{1}{2} J_{\mathbf{Q}} \pm i D^{x}_{\mathbf{Q}}$. Upon Fourier transformation of the spins, the energy of the system becomes

$$E = \frac{1}{2} \beta^2 \mathcal{V} J_0 + \left(1 - \beta^2\right) \mathcal{V} \left[\frac{1}{2} J_{\mathbf{Q}} - \frac{1}{i} \mathbf{D}_{\mathbf{Q}} \cdot \hat{\boldsymbol{t}} \right] + \beta \mathcal{V} \mathbf{B} \cdot \hat{\boldsymbol{t}} \,. \tag{5.18}$$

The addition of the external magnetic field does not change the value of $\mathbf{Q}$, the $\mathbf{q}$-vector which minimizes the energy. It only changes the energy at this $\mathbf{Q}$, which depends on the interactions strengths.

5.2 Local spin fluctuations

Returning to the scenario with no external magnetic field $\mathbf{B} = 0$, the stability of the ground state spin configuration determined in Sec. (5.1.1) can now be investigated by allowing the presence of spin-waves using a classical theory. The ground state spin configuration of unit normalized spins is given by

$$\mathbf{S}_i = \sin(\varphi_i) \hat{\boldsymbol{y}} + \cos(\varphi_j) \hat{\boldsymbol{z}} \,, \tag{5.19}$$

where $\varphi_i = \mathbf{Q} \cdot \mathbf{r}_i$. Introducing local spin fluctuations implies that the spins may deviate from the spin configuration given by Eq. (5.19), and the spin configuration of this excited state can then be described by a new $\mathbf{S}_i$

$$\mathbf{S}_i = \mathbf{S}^0_i + \delta \mathbf{S}_i \tag{5.20}$$

where $\mathbf{S}^0_i$ are the unperturbed spins of the ground state given by Eq. (5.19) and $\delta \mathbf{S}_i$ are the deviations. These deviations can be characterized by a component in each of the two transverse directions of $\mathbf{S}^0_i$, so locally at each lattice site i

$$\mathbf{S}_i = S^0_i \left(\sin(\varphi_i) \hat{\boldsymbol{y}} + \cos(\varphi_i) \hat{\boldsymbol{z}} \right) + S^1_i \left(\cos(\varphi_i) \hat{\boldsymbol{y}} - \sin(\varphi_i) \hat{\boldsymbol{z}} \right) + S^2_i \hat{\boldsymbol{x}} \tag{5.21}$$

where S_i^1 and S_i^2 characterizes the magnitude of the deviation of the spin in each of the two transverse directions, just as in Sec. (3.2.1). The contribution to the spin-wave spectrum from the Heisenberg interaction was determined in Sec. (3.2.1) to be

$$\frac{1}{2}\sum_{ij} J_{ij}\mathbf{S}_i\cdot\mathbf{S}_j \simeq \frac{1}{2}J_{\mathbf{Q}} + \frac{1}{2}\sum_{\mathbf{q}}\left[\left(\frac{1}{2}\left(J_{\mathbf{Q}+\mathbf{q}}+J_{\mathbf{Q}-\mathbf{q}}\right)-J_{\mathbf{Q}}\right)|\pi_{1\mathbf{q}}|^2 + \left(J_{\mathbf{q}}-J_{\mathbf{Q}}\right)|\pi_{2\mathbf{q}}|^2\right]. \tag{5.22}$$

Using the same procedure as in Sec. (3.2.1), the contribution from the DM interaction can now be determined. The cross product between the spin vectors in terms of the spin deviations is

$$\begin{aligned}\mathbf{S}_i\times\mathbf{S}_j = &\left[\left(S_i^0S_j^0+S_i^1S_j^1\right)\sin(\theta_i-\theta_j)+\left(S_i^1S_j^0-S_i^0S_j^1\right)\cos(\theta_i-\theta_j)\right]\hat{\boldsymbol{x}}\\ &\left(S_i^0\cos(\theta_i)-S_i^1\sin(\theta_i)\right)S_j^2-\left[S_i^2\left(S_j^0\cos(\theta_j)-S_j^1\sin(\theta_j)\right)-\right]\hat{\boldsymbol{y}}\\ &\left[S_i^2\left(S_j^0\sin(\theta_j)+S_j^1\cos(\theta_j)\right)-\left(S_i^0\sin(\theta_i)+S_i^1\cos(\theta_i)\right)S_j^2\right]\hat{\boldsymbol{z}}\,.\end{aligned} \tag{5.23}$$

As presented in Sec. (3.2.1), the spin deviations may be parametrized by small fluctuations $\pi_1,\pi_2 \ll 1$ preserving the normalization of the spins

$$\left(S^0,S^1,S^2\right) \simeq \left(1-\frac{1}{2}\left(\pi_1^2+\pi_2^2\right),\pi_1,\pi_2\right). \tag{5.24}$$

The contribution from the DM interaction can then be written as

$$\begin{aligned}H_{\mathrm{DM}} &\equiv \sum_{ij}\mathbf{D}_{ij}\left(\mathbf{S}_i\times\mathbf{S}_j\right)\\ &\simeq \sum_{ij}\mathbf{D}_{ij}\cdot\Bigg(\Bigg[\left(1-\frac{1}{2}\left(\pi_{1i}^2+\pi_{2i}^2+\pi_{1j}^2+\pi_{2j}^2\right)+\pi_{1i}\pi_{1j}\right)\sin\left(\varphi_i-\varphi_j\right)\\ &+\left(\pi_{1i}-\pi_{1j}\right)\cos\left(\varphi_i-\varphi_j\right)\Bigg]\hat{\boldsymbol{x}}+\Big[\pi_{2j}\cos\left(\varphi_i\right)-\pi_{1i}\pi_{2j}\sin\left(\varphi_i\right)-\pi_{2i}\cos\left(\varphi_j\right)\\ &+\pi_{2i}\pi_{1j}\sin\left(\varphi_j\right)\Big]\hat{\boldsymbol{y}}+\left[\pi_{2i}\sin\left(\varphi_j\right)-\pi_{2i}\pi_{1j}\cos\left(\varphi_j\right)-\pi_{2j}\sin\left(\varphi_i\right)+\pi_{1i}\pi_{2j}\cos\left(\varphi_i\right)\right]\hat{\boldsymbol{z}}\Bigg)\end{aligned} \tag{5.25}$$

to second order in the fluctuations. Since the i and j sum over the same sites, the indeces can be relabeled $i\to j$ and $j\to i$ to simplify some terms. Note the antisymmetry of the DM interaction vector $\mathbf{D}_{ji}=-\mathbf{D}_{ij}$. Then

$$\begin{aligned}H_{\mathrm{DM}} \simeq \sum_{ij}\mathbf{D}_{ij}\cdot\Bigg(&\left[\left(1-\pi_{1i}^2-\pi_{2i}^2+\pi_{1i}\pi_{1j}\right)\sin\left(\varphi_i-\varphi_j\right)+2\pi_{1i}\cos\left(\varphi_i-\varphi_j\right)\right]\hat{\boldsymbol{x}}\\ &+\left[-2\pi_{1i}\pi_{2j}\sin\left(\varphi_i\right)-2\pi_{2i}\cos\left(\varphi_j\right)\right]\hat{\boldsymbol{y}}+\left[2\pi_{2i}\sin\left(\varphi_j\right)+2\pi_{1i}\pi_{2j}\cos\left(\varphi_i\right)\right]\hat{\boldsymbol{z}}\Bigg).\end{aligned} \tag{5.26}$$

In the two-dimensional square lattice the DM vector is given by

$$\mathbf{D}_{ij} = \begin{pmatrix} -D\,\mathrm{sgn}\,(y_i - y_j)\,\delta_{z_i,z_j} \\ 0 \\ 0 \end{pmatrix} \tag{5.27}$$

so the y- and z-components of the dot product in Eq. (5.26) vanishes. Upon inserting the Fourier transform of the π's, $\pi_i = \frac{1}{\sqrt{\mathcal{V}}}\sum_{\mathbf{q}} \mathrm{e}^{i\mathbf{q}\cdot\mathbf{r}_i}\pi_{\mathbf{q}}$ and of the DM interaction vector, given by Eq. (2.11), the remaining x-component in reciprocal space is

$$\begin{aligned} H_{\mathrm{DM}} \simeq \frac{1}{\mathcal{V}^2}\sum_{ij}\sum_{\mathbf{q}\mathbf{q}'\mathbf{q}''} D^x_{\mathbf{q}} \mathrm{e}^{i\mathbf{q}\cdot(\mathbf{r}_i-\mathbf{r}_j)} \Bigg\{ \Big[\delta_{\mathbf{q},\mathbf{q}'}\delta_{\mathbf{q},\mathbf{q}''} - \pi_{1\mathbf{q}'}\pi_{1\mathbf{q}''}\mathrm{e}^{i(\mathbf{q}'+\mathbf{q}'')\cdot\mathbf{r}_i} - \pi_{2\mathbf{q}'}\pi_{2\mathbf{q}''}\mathrm{e}^{i(\mathbf{q}'+\mathbf{q}'')\cdot\mathbf{r}_i} \\ + \pi_{1\mathbf{q}'}\pi_{1\mathbf{q}''}\mathrm{e}^{i\mathbf{q}'\cdot\mathbf{r}_i + i\mathbf{q}''\cdot\mathbf{r}_j} \Big] \frac{1}{2i}\left(\mathrm{e}^{i\mathbf{Q}\cdot(\mathbf{r}_i-\mathbf{r}_j)} - \mathrm{e}^{-i\mathbf{Q}\cdot(\mathbf{r}_i-\mathbf{r}_j)}\right) \\ + \delta_{\mathbf{q},\mathbf{q}''}\sqrt{\mathcal{V}}\pi_{1\mathbf{q}'}\mathrm{e}^{i\mathbf{q}'\cdot\mathbf{r}_i}\left(\mathrm{e}^{i\mathbf{Q}\cdot(\mathbf{r}_i-\mathbf{r}_j)} + \mathrm{e}^{-i\mathbf{Q}\cdot(\mathbf{r}_i-\mathbf{r}_j)}\right) \Bigg\} \\ = -iD^x_{\mathbf{Q}} + \sum_{\mathbf{q}} \left[\left(\frac{1}{2}\left(iD^x_{\mathbf{Q}+\mathbf{q}} + iD_{\mathbf{Q}-\mathbf{q}}\right) - iD^x_{\mathbf{Q}} \right) |\pi_{1\mathbf{q}}|^2 - iD^x_{\mathbf{Q}}|\pi_{2\mathbf{q}}|^2 \right] . \end{aligned} \tag{5.28}$$

Combining this with the contribution from the Heisenberg exchange interaction in Eq. (5.22) yields a Hamiltonian with two modes

$$H \simeq \frac{1}{2}J_{\mathbf{Q}} - iD^x_{\mathbf{Q}} + \sum_{\mathbf{q}} \left(\omega_{1\mathbf{q}}|\pi_{1\mathbf{q}}|^2 + \omega_{2\mathbf{q}}|\pi_{2\mathbf{q}}|^2\right) \tag{5.29}$$

where

$$\omega_{1\mathbf{q}} = \frac{1}{4}\left(J_{\mathbf{Q}+\mathbf{q}} + J_{\mathbf{Q}-\mathbf{q}} + 2iD^x_{\mathbf{Q}+\mathbf{q}} + 2iD^x_{\mathbf{Q}-\mathbf{q}}\right) - \frac{1}{2}J_{\mathbf{Q}} - iD^x_{\mathbf{Q}} \tag{5.30}$$

$$\omega_{2\mathbf{q}} = \frac{1}{2}\left(J_{\mathbf{q}} - J_{\mathbf{Q}}\right) - iD^x_{\mathbf{Q}}\,. \tag{5.31}$$

As conducted in Sec. (3.2.3) the π-fields can be quantized analogously. As the Hamiltonian in Eq. (5.29) and Eq. (3.21), have the same form with a constant term and sum over $\mathbf{q}$-vectors quadratic in the π-fields, the derivation of the quantization of the fluctuations is exactly the same in the two cases. Therefore, the Hamiltonian in Eq. (5.29) can be written as

$$H = \frac{1}{2}J_{\mathbf{Q}} - iD^x_{\mathbf{Q}} + \sum_{\mathbf{q}} \hbar\Omega_{\mathbf{q}}\left(a^\dagger_{\mathbf{q}}a_{\mathbf{q}} + \frac{1}{2}\right) \tag{5.32}$$

where the second quantized spin-wave operators are

$$a_{\mathbf{q}} = \frac{1}{\sqrt{2}}\left(\frac{1}{c_{\mathbf{q}}}x_{\mathbf{q}} + \frac{i}{\hbar}c_{\mathbf{q}}p_{\mathbf{q}}\right), \qquad a^\dagger_{-\mathbf{q}} = \frac{1}{\sqrt{2}}\left(\frac{1}{c_{\mathbf{q}}}x_{\mathbf{q}} - \frac{i}{\hbar}c_{\mathbf{q}}p_{\mathbf{q}}\right) \tag{5.33}$$

where $c_{\mathbf{q}} = \sqrt{\frac{\hbar\sqrt{\omega_{2\mathbf{q}}}}{\sqrt{\omega_{1\mathbf{q}}}}}$. The spin-wave spectrum is once again

$$\Omega_{\mathbf{q}} = \sqrt{\omega_{1\mathbf{q}}\omega_{2\mathbf{q}}}\,. \tag{5.34}$$

Denoting $\xi_x = \cos(xa)$ and $\bar{\xi}_x = \sin(xa)$, the symmetric exchange interaction from Eq. (3.10) and the antisymmetric exchange interaction from Eq. (5.13) can be written as

$$J_{\mathbf{q}} = 2J_1\left(\xi_{q_y} + \xi_{q_z}\right) + 4J_2\xi_{q_y}\xi_{q_z} \tag{5.35}$$
$$D^x_{\mathbf{q}} = 2iD\bar{\xi}_{q_y}\,. \tag{5.36}$$

Since $\mathbf{Q} = (Q_y, Q_z) = \left(Q_y, \frac{\pi}{a}\right)$ it can be seen that

$$J_{\mathbf{Q}} = 2J_1\left(\xi_{Q_y} - 1\right) - 4J_2\xi_{Q_y} \tag{5.37}$$
$$J_{\mathbf{Q}\pm\mathbf{q}} = 2J_1\left(\xi_{Q_y\pm q_y} - \xi_{q_z}\right) - 4J_2\xi_{Q_y\pm q_y}\xi_{q_z} \tag{5.38}$$
$$-2iD_{\mathbf{Q}} = 4D\bar{\xi}_{Q_y} \tag{5.39}$$
$$2iD_{\mathbf{Q}\pm\mathbf{q}} = -4D\bar{\xi}_{Q_y\pm q_y} \tag{5.40}$$

using $\cos(\pi \pm x) = -\cos(x)$. The spin-wave spectrum from Eq. (5.34) is then

$$\begin{aligned}\Omega =&\sqrt{J_1\left(\xi_{Q_y}\xi_{q_y} - \xi_{q_z} - \xi_{Q_y} + 1\right) + 2J_2\xi_{Q_y}\left(1 - \xi_{q_y}\xi_{q_z}\right) + 2D\bar{\xi}_{Q_y}\left(1 - \xi_{q_y}\right)}\\ &\sqrt{J_1\left(\xi_{q_y} + \xi_{q_z} + 1 - \xi_{Q_y}\right) + 2J_2\left(\xi_{q_y}\xi_{q_z} + \xi_{Q_y}\right) + 2D\bar{\xi}_{Q_y}}\,.\end{aligned} \tag{5.41}$$

Plots of the spectrum can be seen in the following section, see Fig (5.4) and Fig. (5.5).

5.3 Quantum spin fluctuations

Similarly to what was done for the J_1-J_2 Heisenberg model in Sec. (3.3), a quantum mechanical treatment of spin fluctuations will now be carried out in the J_1-J_2 Heisenberg model with the addition of the DM interaction. Since the ground state spin configuration is altered when the DM interaction is added, the results from Sec. (3.3) cannot be reused and this part of the calculation has to be done once more.

5.3.1 Holstein-Primakoff transformation

Analogously to what was done for the J_1-J_2 Heisenberg model in Sec. (3.3.1), the Holstein-Primakoff transformation will once again be employed to obtain a Hamiltonian expressed in terms of the magnon creation and annihilation operators in second quantization. In the large spin S limit, the Holstein-Primakoff transformation is given by Eqs. (3.62)-(3.64). Using the J_1-J_2 Heisenberg model with the addition of the DM interaction, the Hamiltonian is given by Eq. (5.1). The Holstein-Primakoff representations are given

in local coordinate systems, in which the spins are parallel to the z-axis. The ground state spin configuration of the Hamiltonian in Eq. (5.1) is an antiferromagnetic stripe in the z-direction and a spiral in the y-direction. Since the spins lie in the yz-plane, a rotation around the x-axis will once again be sufficient to align all spins with the z-axis. In Sec. (3.3.1) it was shown how this method works on the Heisenberg model. Since the DM interaction couples to the cross product of the spins, the method differs slightly in this model. Utilizing the orthorgonality of the rotation matrices $R_x^{\mathrm{T}} R_x = R_x^{-1} R_x = \mathbb{1}$ and the feature $R_x^{-1}(\theta) = R_x(-\theta)$, with R_x given by Eq. (3.65), the cross product between the spin projection operators can be written as

$$\begin{aligned} \mathbf{D}_{ij} \cdot (\mathbf{S}_i \times \mathbf{S}_j) &= \mathbf{D}_{ij} \cdot \left(\mathbf{S}_i \left[R_x^{-1}(\theta_i) R_x(\theta_i) \right] \times \left[R_x^{-1}(\theta_j) R_x(\theta_j) \right] \mathbf{S}_j \right) \\ &= \mathbf{D}_{ij} \cdot \left(\left(\tilde{\mathbf{S}}_i R_x(\theta_i) \right) \times \left(R_x(-\theta_j) \tilde{\mathbf{S}}_j \right) \right) \end{aligned} \tag{5.42}$$

where $\tilde{\mathbf{S}}_{i,j}$ are the spin operators defined in the local reference frame. Carrying out the matrix multiplication with R_x, given by Eq. (3.65), yields

$$\begin{aligned} &\mathbf{D}_{ij} \cdot \left(\left(\tilde{\mathbf{S}}_i R_x(\theta_i) \right) \times \left(R_x(-\theta_j) \tilde{\mathbf{S}}_j \right) \right) \\ &= D_{ij}^x \Big\{ \left[\cos(\theta_i) \tilde{S}_i^y + \sin(\theta_i) \tilde{S}_i^z \right] \left[\sin(-\theta_j) \tilde{S}_j^y + \cos(-\theta_j) \tilde{S}_j^z \right] \\ &- \left[-\sin(\theta_i) \tilde{S}_i^y + \cos(\theta_i) \tilde{S}_i^z \right] \left[\cos(-\theta_j) \tilde{S}_j^y - \sin(-\theta_j) \tilde{S}_j^z \right] \Big\} \\ &+ D_{ij}^y \left\{ -\tilde{S}_i^x \left(\sin(-\theta_j) \tilde{S}_j^y + \cos(-\theta_j) \tilde{S}_j^z \right) + \left(-\sin(\theta_i) \tilde{S}_i^y + \cos(\theta_i) \tilde{S}_i^z \right) \tilde{S}_j^x \right\} \\ &+ D_{ij}^z \left\{ \tilde{S}_i^x \left(\cos(-\theta_j) \tilde{S}_j^y - \sin(-\theta_j) \tilde{S}_j^z \right) - \left(\cos(\theta_i) \tilde{S}_i^y + \sin(\theta_i) \tilde{S}_i^z \right) \tilde{S}_j^x \right\} . \end{aligned} \tag{5.43}$$

In the large S limit the Holstein-Primakoff representations can now be inserted. Utilizing relabelling of indeces $i \to j$ and $j \to i$, and being careful with the symmetries of the trigonometric functions yields a DM Hamiltonian given by

$$\begin{aligned} H_{\mathrm{DM}} &= \sum_{ij} \mathbf{D}_{ij} \cdot (\mathbf{S}_i \times \mathbf{S}_j) \\ &\simeq \sum_{ij} \Bigg[D_{ij}^x \Big\{ -i\sqrt{2S} S \cos(\theta_i - \theta_j) \left(-b_i^\dagger + b_i \right) \\ &+ S \sin(\theta_i - \theta_j) \left(\frac{1}{2} \left[-b_i^\dagger b_j^\dagger - b_i b_j \right] + b_i^\dagger b_j + S - 2 b_i^\dagger b_i \right) \Big\} \\ &+ D_{ij}^y \left\{ -iS \sin(\theta_i) \left(b_i b_j - b_i^\dagger b_j^\dagger - b_i b_j^\dagger + b_i^\dagger b_j \right) - i\sqrt{2S} S \cos(\theta_i) \left(b_j + b_j^\dagger \right) \right\} \\ &+ D_{ij}^z \left\{ -iS \cos(\theta_i) \left(-b_i b_j + b_i^\dagger b_j^\dagger - b_i b_j^\dagger + b_i^\dagger b_j \right) - i\sqrt{2S} S \sin(\theta_i) \left(b_j + b_j^\dagger \right) \right\} \Bigg] , \end{aligned} \tag{5.44}$$

to second order in the magnon creation and annihilation operators, since

$$\mathbf{D}_{ji} = -\mathbf{D}_{ij}\,. \tag{5.45}$$

As the DM vector $\mathbf{D}_{ij}$ only has a x-component for the two-dimensional square lattice, see Eq. (5.7), $D^y_{ij} = D^z_{ij} = 0$. The DM Hamiltonian can be simplified further as a result of this. Combining this with the Hamiltonian for the Heisenberg model, obtained in Sec. (3.3.1), given by Eq. (3.70) yields the full Hamiltonian describing the Heisenberg model with present DM interaction in the two-dimensional square lattice, which is given by

$$\begin{aligned} H \simeq \frac{S}{2}\sum_{ij} J_{ij}\Bigg\{ & 2\cos^2\left(\frac{\theta_i-\theta_j}{2}\right) b_i^\dagger b_j + \sin^2\left(\frac{\theta_i-\theta_j}{2}\right)\left(b_i^\dagger b_j^\dagger + b_i b_j\right) - 2\cos\left(\theta_i-\theta_j\right) b_i^\dagger b_i \\ & + S\cos\left(\theta_i-\theta_j\right) + 2\sin\left(\theta_i-\theta_j\right) i\sqrt{\frac{S}{2}}\left(b_i^\dagger - b_i\right)\Bigg\} \\ & + \sum_{ij} D^x_{ij}\Bigg\{ - i\sqrt{2S}S\cos(\theta_i-\theta_j)\left(-b_i^\dagger + b_i\right) \\ & + S\sin(\theta_i-\theta_j)\left(\frac{1}{2}\left[-b_i^\dagger b_j^\dagger - b_i b_j\right] + b_i^\dagger b_j + S - 2b_i^\dagger b_i\right)\Bigg\}\,. \end{aligned} \tag{5.46}$$

Now, the Fourier transform of the Holstein-Primakoff bosons, given by Eq. (3.71) and Eq. (3.72), will be inserted in the Hamiltonian, and the nearest and next-nearest neighbor contributions will be calculated separately. This will be done in detail, as one might quickly lose track of the contribution that each term in the Hamiltonian yields.

Nearest neighbor contribution

The ground state spin configuration consists of spins rotating by π along the z-axis and spiraling by some angle ϕ in the y-direction, see Fig. (5.3).

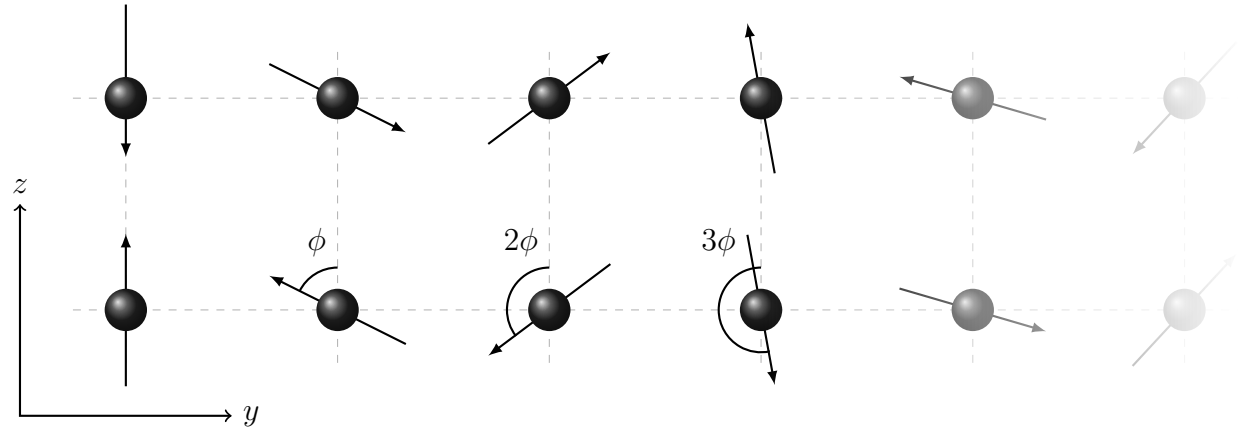

Figure 5.3: Ground state spin configuration in J_1-J_2 Heisenberg model with DM interaction, for $J_1 = J_2 = D = 1$ with an antiferromagnetic stripe in z-direction and spiral varying with angle ϕ in y-direction.

The difference in angle between a site i and its nearest neighbor j is then

$$\theta_i - \theta_j = \begin{cases} \phi & \text{for a nearest neighbors in the } +y\text{-direction,} \\ -\phi & \text{for a nearest neighbor in the } -y\text{-direction,} \\ \pm\pi & \text{for nearest neighbors in the } z\text{-direction.} \end{cases} \tag{5.47}$$

Consider then a term like

$$\begin{aligned} S\sum_{\langle ij\rangle} J_{ij}\cos^2\left(\frac{\theta_i-\theta_j}{2}\right) b_i^\dagger b_j &= \frac{S}{\mathcal{V}} J_1 \sum_{\langle ij\rangle}\sum_{\mathbf{q}\mathbf{q}'} \cos^2\left(\frac{\theta_i-\theta_j}{2}\right) \mathrm{e}^{-i\mathbf{q}\cdot\mathbf{r}_i}\mathrm{e}^{i\mathbf{q}'\cdot\mathbf{r}_j} b_{\mathbf{q}}^\dagger b_{\mathbf{q}'} \\ &= \frac{S}{\mathcal{V}} J_1 \sum_{i\mathbf{q}\mathbf{q}'} \mathrm{e}^{-i(\mathbf{q}-\mathbf{q}')\cdot\mathbf{r}_i}\Bigg(\cos^2\left(\frac{\phi}{2}\right)\left[\mathrm{e}^{iq_y'a}+\mathrm{e}^{-iq_y'a}\right] \\ &\quad + \cos^2\left(\frac{\pi}{2}\right)\left[\mathrm{e}^{iq_z'a}+\mathrm{e}^{-iq_z'a}\right]\Bigg) b_{\mathbf{q}}^\dagger b_{\mathbf{q}'} \\ &= 2SJ_1\sum_{\mathbf{q}}\cos^2\left(\frac{\phi}{2}\right)\cos(q_y a) b_{\mathbf{q}}^\dagger b_{\mathbf{q}} \\ &= SJ_1\sum_{\mathbf{q}}\cos^2\left(\frac{\phi}{2}\right)\cos(q_y a)\left(b_{\mathbf{q}}^\dagger b_{\mathbf{q}} + b_{-\mathbf{q}}^\dagger b_{-\mathbf{q}}\right) \end{aligned} \tag{5.48}$$

where $\sum_{\mathbf{q}} b_{\mathbf{q}}^\dagger b_{\mathbf{q}} = \sum_{\mathbf{q}} b_{-\mathbf{q}}^\dagger b_{-\mathbf{q}}$ was utilized and $\sum_{\langle ij\rangle}$ once again denotes a sum over nearest neighboring sites. In a similar manner it can be seen that

$$\begin{aligned} &\frac{S}{2}\sum_{\langle ij\rangle} J_{ij}\sin^2\left(\frac{\theta_i-\theta_j}{2}\right)\left(b_i^\dagger b_j^\dagger + b_i b_j\right) \\ &= \frac{S}{2\mathcal{V}} J_1 \sum_{\langle ij\rangle}\sum_{\mathbf{q}\mathbf{q}'} \sin^2\left(\frac{\theta_i-\theta_j}{2}\right)\left(\mathrm{e}^{-i\mathbf{q}\cdot\mathbf{r}_i}\mathrm{e}^{-i\mathbf{q}'\cdot\mathbf{r}_j} b_{\mathbf{q}}^\dagger b_{\mathbf{q}'}^\dagger + \mathrm{e}^{i\mathbf{q}\cdot\mathbf{r}_i}\mathrm{e}^{i\mathbf{q}'\cdot\mathbf{r}_j} b_{\mathbf{q}} b_{\mathbf{q}'}\right) \\ &= SJ_1\sum_{\mathbf{q}}\left(\sin^2\left(\frac{\phi}{2}\right)\cos(q_y a)+\cos(q_z a)\right)\left(b_{\mathbf{q}}^\dagger b_{-\mathbf{q}}^\dagger + b_{\mathbf{q}} b_{-\mathbf{q}}\right) \end{aligned} \tag{5.49}$$

and

$$\begin{aligned} -S\sum_{\langle ij\rangle} J_{ij}\cos\left(\theta_i-\theta_j\right) b_i^\dagger b_i &= -\frac{SJ_1}{\mathcal{V}}\sum_{\langle ij\rangle}\sum_{\mathbf{q}\mathbf{q}'}\cos\left(\theta_i-\theta_j\right)\mathrm{e}^{-i(\mathbf{q}-\mathbf{q}')\cdot\mathbf{r}_i} b_{\mathbf{q}}^\dagger b_{\mathbf{q}'} \\ &= -SJ_1\sum_{\mathbf{q}} 2\left(\cos(\phi)-1\right) b_{\mathbf{q}}^\dagger b_{\mathbf{q}} \\ &= 2SJ_1\sum_{\mathbf{q}}\sin^2\left(\frac{\phi}{2}\right)\left(b_{\mathbf{q}}^\dagger b_{\mathbf{q}} + b_{-\mathbf{q}}^\dagger b_{-\mathbf{q}}\right) \end{aligned} \tag{5.50}$$

which was rewritten using the trigonometric identity $(\cos(x)-1) = -2\sin^2\left(\frac{x}{2}\right)$. For Heisenberg terms linear in the bosonic operators, it can be seen that

$$\begin{aligned}\sum_{\langle ij\rangle} J_{ij}\sin(\theta_i-\theta_j)b_i^\dagger &= \frac{1}{\sqrt{\mathcal{V}}}J_1\sum_{\langle ij\rangle}\sum_{\mathbf{q}}\sin(\theta_i-\theta_j)\mathrm{e}^{-i\mathbf{q}\cdot\mathbf{r}_i}b_{\mathbf{q}}^\dagger \\ &= \frac{1}{\sqrt{\mathcal{V}}}J_1\sum_{i\mathbf{q}}\mathrm{e}^{-i\mathbf{q}\cdot\mathbf{r}_i}\left[2\sin(\pi)+\sin(\phi)+\sin(-\phi)\right]b_{\mathbf{q}}^\dagger \\ &= 0\,.\end{aligned} \tag{5.51}$$

For the DM terms linear in the magnon creation and annihilation operators, it can similarly be seen that

$$\begin{aligned}\sum_{ij} D_{ij}^x\cos(\theta_i-\theta_j)b_i^\dagger &= \frac{1}{\sqrt{\mathcal{V}}}\sum_{ij}\sum_{\mathbf{q}} D_{ij}^x\cos(\theta_i-\theta_j)\mathrm{e}^{-i\mathbf{q}\cdot\mathbf{r}_i}b_{\mathbf{q}}^\dagger \\ &= \frac{1}{\sqrt{\mathcal{V}}}\sum_{i\mathbf{q}}\mathrm{e}^{i\mathbf{q}\cdot\mathbf{r}_i}b_{\mathbf{q}}^\dagger\left(D\cos(-\phi)-D\cos(\phi)\right) \\ &= 0\,.\end{aligned} \tag{5.52}$$

The mixed DM terms yields

$$\begin{aligned}S\sum_{ij} D_{ij}^x\sin(\theta_i-\theta_j)b_i^\dagger b_j &= \frac{S}{\mathcal{V}}\sum_{ij}\sum_{\mathbf{q},\mathbf{q}'} D_{ij}^x\sin(\theta_i-\theta_j)\mathrm{e}^{-i\mathbf{q}\cdot\mathbf{r}_i}\mathrm{e}^{i\mathbf{q}'\cdot\mathbf{r}_j}b_{\mathbf{q}}^\dagger b_{\mathbf{q}'} \\ &= \frac{S}{\mathcal{V}}\sum_{i\mathbf{q}\mathbf{q}'}\mathrm{e}^{-i(\mathbf{q}-\mathbf{q}')\cdot\mathbf{r}_i}\left(D\sin(-\phi)\mathrm{e}^{iq_y'a}-D\sin(\phi)\mathrm{e}^{-iq_y'a}\right)b_{\mathbf{q}}^\dagger b_{\mathbf{q}'} \\ &= -S\sum_{\mathbf{q}} D\sin(\phi)\cos(q_y a)\left(b_{\mathbf{q}}^\dagger b_{\mathbf{q}}+b_{-\mathbf{q}}^\dagger b_{-\mathbf{q}}\right)\end{aligned} \tag{5.53}$$

and the procedure is completely analogous for the $b_i^\dagger b_j^\dagger$ and the $b_i b_j$ DM terms. The nearest neighbor contribution from the constant term is

$$\frac{S^2}{2}\sum_{\langle ij\rangle} J_{ij}\cos\left(\theta_i-\theta_j\right) = \frac{S^2}{2}J_1\sum_i\left(2\cos(\pi)+2\cos(\phi)\right) = -2NS^2J_1\sin^2\left(\frac{\phi}{2}\right)\,. \tag{5.54}$$

Lastly, the remaining DM term is

$$\begin{aligned}-2S\sum_{ij} D_{ij}^x\sin(\theta_i-\theta_j)b_i^\dagger b_i &= -\frac{2S}{\mathcal{V}}\sum_{ij}\sum_{\mathbf{q},\mathbf{q}'} D_{ij}^x\sin(\theta_i-\theta_j)\mathrm{e}^{-i(\mathbf{q}-\mathbf{q}')\cdot\mathbf{r}_i}b_{\mathbf{q}}^\dagger b_{\mathbf{q}'} \\ &= -\frac{2S}{\mathcal{V}}\sum_{i\mathbf{q}\mathbf{q}'}\mathrm{e}^{-i(\mathbf{q}-\mathbf{q}')\cdot\mathbf{r}_i}\left(D\sin(-\phi)-D\sin(\phi)\right)b_{\mathbf{q}}^\dagger b_{\mathbf{q}'} \\ &= 2S\sum_{\mathbf{q}} D\sin(\phi)\left(b_{\mathbf{q}}^\dagger b_{\mathbf{q}}+b_{-\mathbf{q}}^\dagger b_{-\mathbf{q}}\right)\,.\end{aligned} \tag{5.55}$$

As the nearest-neighbor contributions have now been determined, the next-nearest neighbor contributions will now be considered.

Next-nearest neighbor contribution

The angle between a site i and its next nearest neighbor j is

$$\theta_i - \theta_j = \begin{cases} -\phi \pm \pi & \text{for a next-nearest neighbor in } +y\text{-direction,} \\ \phi \pm \pi & \text{for a next-nearest neighbor in } -y\text{-direction.} \end{cases} \tag{5.56}$$

There is no DM interaction between next-nearest neighbors. Consider again the term

$$\begin{aligned} S \sum_{\langle\langle ij \rangle\rangle} J_{ij} \cos^2\left(\frac{\theta_i - \theta_j}{2}\right) b_i^\dagger b_j &= \frac{SJ_2}{\mathcal{V}} \sum_{\langle\langle ij \rangle\rangle} \sum_{\mathbf{q}\mathbf{q}'} \sin^2\left(\frac{\phi}{2}\right) \mathrm{e}^{-i\mathbf{q}\cdot\mathbf{r}_i} \mathrm{e}^{i\mathbf{q}'\cdot\mathbf{r}_j} b_{\mathbf{q}}^\dagger b_{\mathbf{q}'} \\ &= \frac{SJ_2}{\mathcal{V}} \sum_{i\mathbf{q}\mathbf{q}'} \sin^2\left(\frac{\phi}{2}\right) \mathrm{e}^{-i(\mathbf{q}-\mathbf{q}')\cdot\mathbf{r}_i} \Big(\mathrm{e}^{i\left(q_y' a + q_z' a\right)} + \mathrm{e}^{i\left(q_y' a - q_z' a\right)} \\ &\quad + \mathrm{e}^{i\left(-q_y' a + q_z' a\right)} + \mathrm{e}^{-i\left(q_y' a + q_z' a\right)} \Big) b_{\mathbf{q}}^\dagger b_{\mathbf{q}'} \\ &= 2SJ_2 \sum_{\mathbf{q}} \sin^2\left(\frac{\phi}{2}\right) \cos\left(q_y a\right) \cos\left(q_z a\right) \left(b_{\mathbf{q}}^\dagger b_{\mathbf{q}} + b_{-\mathbf{q}}^\dagger b_{-\mathbf{q}} \right) \end{aligned} \tag{5.57}$$

where $\sum_{\langle\langle ij \rangle\rangle}$ denotes a sum over next-nearest neighboring sites only. Similarly

$$\begin{aligned} &\frac{S}{2} \sum_{\langle\langle ij \rangle\rangle} J_{ij} \sin^2\left(\frac{\theta_i - \theta_j}{2}\right) \left(b_i^\dagger b_j^\dagger + b_i b_j \right) \\ &= 2SJ_2 \sum_{\mathbf{q}} \cos^2\left(\frac{\phi}{2}\right) \cos\left(q_y a\right) \cos\left(q_z a\right) \left(b_{\mathbf{q}}^\dagger b_{-\mathbf{q}}^\dagger + b_{\mathbf{q}} b_{-\mathbf{q}} \right) \end{aligned} \tag{5.58}$$

and

$$-SJ_2 \sum_{\langle\langle ij \rangle\rangle} \cos\left(\theta_i - \theta_j\right) b_i^\dagger b_i = 2SJ_2 \sum_{\mathbf{q}} \cos(\phi) \left(b_{\mathbf{q}}^\dagger b_{\mathbf{q}} + b_{-\mathbf{q}}^\dagger b_{-\mathbf{q}} \right) . \tag{5.59}$$

The linear term of the Hamiltonian vanishes once again, since

$$\sum_{\langle\langle ij \rangle\rangle} J_{ij} \sin(\theta_i - \theta_j) b_i^\dagger = J_2 \sum_i \left(2\sin(\phi) - 2\sin(\phi) \right) b_i^\dagger = 0 . \tag{5.60}$$

Lastly the contribution from the constant term is

$$\frac{S^2}{2} \sum_{\langle\langle ij \rangle\rangle} J_{ij} \cos\left(\theta_i - \theta_j\right) = -\frac{S^2}{2} J_2 \sum_i 4\cos\left(\phi\right) = -2S^2 J_2 N \cos(\phi) . \tag{5.61}$$

5.3.2 Bosonic Bogoliubov transformation

Collecting all terms from the nearest and next-nearest neighbor contributions, it can be seen that the full Hamiltonian in Eq. (5.46) can be written on a bilinear form

$$H = \mathcal{C} + \sum_{\mathbf{q}} \left[\mathcal{E}_0 \left(b^\dagger_{\mathbf{q}} b_{\mathbf{q}} + b^\dagger_{-\mathbf{q}} b_{-\mathbf{q}} \right) + \mathcal{E}_1 \left(b^\dagger_{\mathbf{q}} b^\dagger_{-\mathbf{q}} + b_{\mathbf{q}} b_{-\mathbf{q}} \right) \right] \tag{5.62}$$

where

$$\mathcal{C} = -2NS^2 \left(J_2 \cos(\phi) + J_1 \sin^2 \left(\frac{\phi}{2} \right) \right) \tag{5.63}$$

$$\begin{aligned} \frac{\mathcal{E}_0}{S} = {} & J_1 \cos^2 \left(\frac{\phi}{2} \right) \cos(q_y a) + 2J_1 \sin^2 \left(\frac{\phi}{2} \right) + 2J_2 \sin^2 \left(\frac{\phi}{2} \right) \cos\left(q_y a\right) \cos\left(q_z a\right) \\ & + 2J_2 \cos(\phi) - D \sin(\phi) \cos(q_y a_y) + 2D \sin(\phi) \end{aligned} \tag{5.64}$$

$$\begin{aligned} \frac{\mathcal{E}_1}{S} = {} & J_1 \sin^2 \left(\frac{\phi}{2} \right) \cos(q_y a) + J_1 \cos(q_z a) + 2J_2 \cos^2 \left(\frac{\phi}{2} \right) \cos\left(q_y a\right) \cos\left(q_z a\right) \\ & + D \sin(\phi) \cos(q_y a) \,. \end{aligned} \tag{5.65}$$

The Hamiltonian for the J_1-J_2 Heisenberg model with added DM interaction in the Holstein-Primakoff representation in Eq. (5.62) is of exactly the same form as the one for the J_1-J_2 Heisenberg model in Eq. (3.86). Therefore, the procedure to diagonalize the Hamiltonian and obtain the eigenvalues $\omega_{\mathbf{q}}$ of the system using the Bogoliubov transformation is exactly the same as in Sec. (3.3.2), and the result can then readily be read of

$$\Omega_{\mathbf{q}} = \sqrt{\left(\mathcal{E}_0\right)^2 - \left(\mathcal{E}_1\right)^2} \,. \tag{5.66}$$

The angle ϕ is actually $\phi = Q_y$, which is evident when considering the dot product $\mathbf{S}_i \cdot \mathbf{S}_j$ (with spins given by Eq. (5.19)) between the two spins at $\mathbf{r}_i = (0,0)$ and $\mathbf{r}_j = (1,0)$ in the lattice. This yields $\mathbf{S}_i \cdot \mathbf{S}_j = \cos\left(Q_y\right)$, making $\phi = Q_y$. Inserting $\mathcal{E}_0$ and $\mathcal{E}_1$ and utilizing the trigonometric identities $2\cos^2\left(\frac{x}{2}\right) = 1 + \cos(x)$ and $2\sin^2\left(\frac{x}{2}\right) = 1 - \cos(x)$ yields a spin-wave spectrum of

$$\begin{aligned} \Omega_{\mathbf{q}} = \Bigg[& \left(\frac{1}{2} J_1 \xi_{q_y} \left(1 + \xi_{Q_y}\right) + J_1 \left(1 - \xi_{Q_y}\right) + J_2 \left(1 - \xi_{Q_y}\right) \xi_{q_y} \xi_{q_z} + 2J_2 \xi_{Q_y} - D \bar{\xi}_{Q_y} \xi_{q_y} + 2D \bar{\xi}_{Q_y} \right)^2 \\ & - \left(\frac{1}{2} J_1 \left(1 - \xi_{Q_y}\right) \xi_{q_y} + J_1 \xi_{q_z} + J_2 \left(1 + \xi_{Q_y}\right) \xi_{q_y} \xi_{q_z} + D \bar{\xi}_{Q_y} \xi_{q_y} \right)^2 \Bigg]^{\frac{1}{2}} . \end{aligned} \tag{5.67}$$

The difference between to squared terms, as is seen in Eq. (5.67), can be written as $A^2 - B^2 = (A + B)(A - B)$. Using this, the spin-wave spectrum becomes

$$\begin{aligned} \Omega_{\mathbf{q}} = {} & \sqrt{J_1 \left(\xi_{Q_y} \xi_{q_y} - \xi_{q_z} - \xi_{Q_y} + 1 \right) + 2J_2 \xi_{Q_y} \left(1 - \xi_{q_y} \xi_{q_z}\right) + 2D \bar{\xi}_{Q_y} \left(1 - \xi_{q_y}\right)} \\ & \sqrt{J_1 \left(\xi_{q_y} + \xi_{q_z} + 1 - \xi_{Q_y} \right) + 2J_2 \left(\xi_{q_y} \xi_{q_z} + \xi_{Q_y} \right) + 2D \bar{\xi}_{Q_y}} \,. \end{aligned} \tag{5.68}$$

Comparing Eq. (5.68) and Eq. (5.34), it can be seen that the exact same spin-wave spectrum is obtained by using a classical spin-wave theory, as by using a quantum mechanical approach. The dispersion can be seen for different interaction strengths in Fig. (5.4) and Fig. (5.5).

In the limit of no DM interaction $\mathbf{D}_i j = 0$ the y-component of the minimal $\mathbf{q}$-vector $Q_y = \tan^{-1}\left(\frac{2D}{2J_2 - J_2}\right)$ is $Q_y = 0$ and the spin-wave dispersion in Eq. (5.68) reduces to the J_1-J_2 Heisenberg model spin-wave dispersion in Eq. (3.94) with $\Theta = 0$. This unsurprisingly amounts to picking $\mathbf{Q}^{(1)}$ as the minimal $\mathbf{q}$-vector (rather than $\mathbf{Q}^{(2)}$) which is exactly what the addition of the DM interaction amounts to.

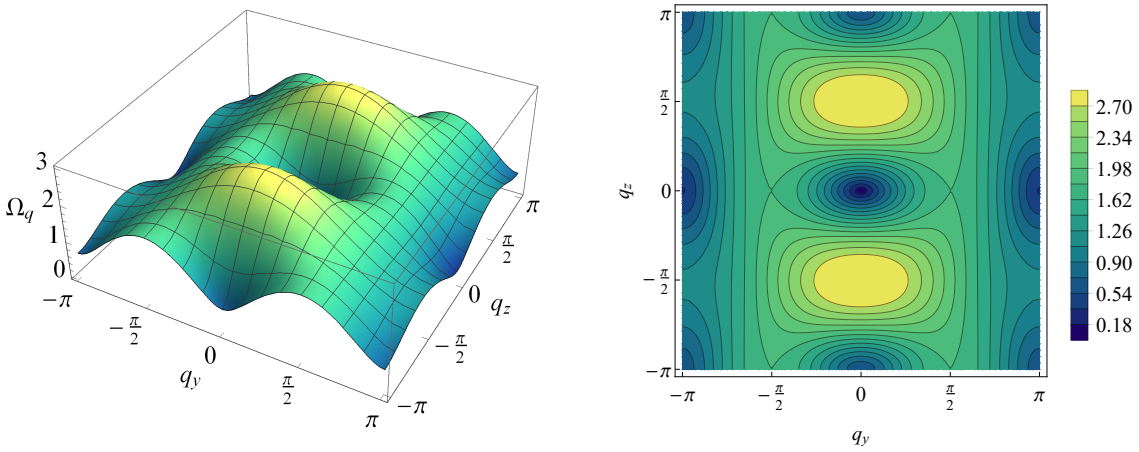

(a) 3D plot of $\Omega_{\mathbf{q}}$.

(b) Contour plot of $\Omega_{\mathbf{q}}$.

Figure 5.4: A 3D and a contour plot of the spin-wave dispersion $\Omega_{\mathbf{q}}$ from Eq. (5.68) for $J_1 = 1$, $J_2 = 1$ and $D = 0.2$ on the two-dimensional square lattice.

In Fig. (5.4) the effect of adding the DM interaction can be seen, as it describes the same situation as Fig. (3.5a) but with DM interaction. The addition of the DM interaction raises the energy of the points on the edge of the Brillouin Zone. In Fig. (5.5) the effect of adding the DM interaction at the highly frustrated point of the J_1-J_2 Heisenberg model (see Fig. (3.7a)) can be seen. The lines of zero-energy modes have been erased, as the energy is raised in every point except for the Γ-point.

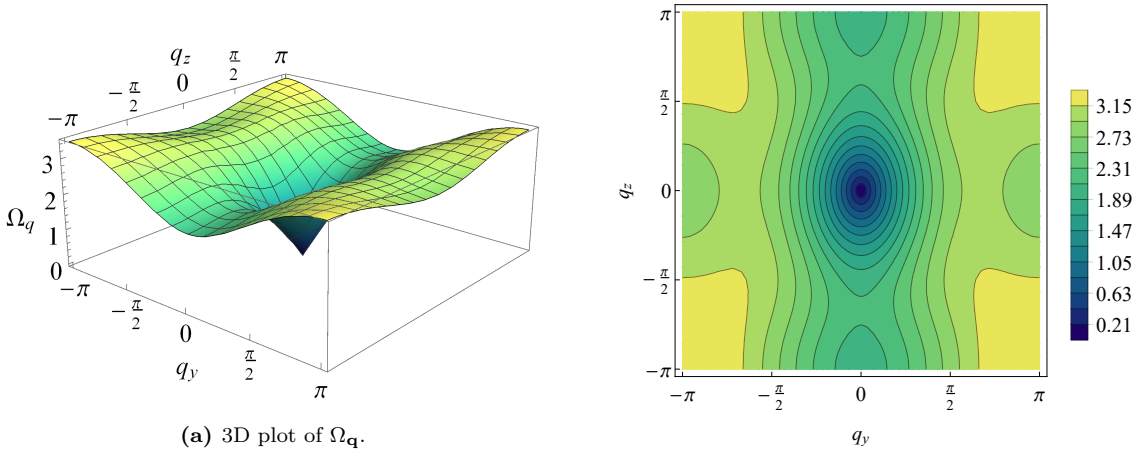

(a) 3D plot of $\Omega_{\mathbf{q}}$.

(b) Contour plot of $\Omega_{\mathbf{q}}$.

Figure 5.5: A 3D and a contour plot of the spin-wave dispersion $\Omega_{\mathbf{q}}$ from Eq. (5.68) for $J_1 = 1$, $J_2 = 0.5$ and $D = 1$ on the two-dimensional square lattice.

Group velocities near Γ-point

The group velocities of the low-energy modes in the spectrum given by Eq. (5.68) can now be investigated. These clearly lie near the center of the Brillouin Zone, the so-called Γ-point, see Fig. (5.5). The spin-wave spectrum is therefore expanded numerically in $\mathbf{q} = (q_y, q_z)$ to second order in $\mathbf{q}$. The spin-wave dispersion becomes

$$\begin{aligned} \Omega_{\mathbf{q}} &\simeq \sqrt{\Delta_y q_y^2 + \Delta_z q_z^2} \\ &= \sqrt{q^2 \left(\Delta_y \cos^2(\theta) + \Delta_z \sin^2(\theta)\right)} \end{aligned} \tag{5.69}$$

when changing from cartesian to polar coordinates $q_y = q\cos(\theta)$ and $q_z = q\sin(\theta)$. Here

$$\Delta_y = \frac{1}{2}\left(J_1\xi_{Q_y} - 2J_2\xi_{Q_y} - 2D\bar{\xi}_{Q_y}\right)\left(-3J_1 + J_1\xi_{Q_y} - 2J_2\xi_{Q_y} - 2J_2 - 2D\bar{\xi}_{Q_y}\right) \tag{5.70}$$

$$\Delta_z = \frac{1}{2}\left(J_1 + 2J_2\xi_{Q_y}\right)\left(3J_1 - J_1\xi_{Q_y} + 2J_2\xi_{Q_y} + 2J_2 + 2D\bar{\xi}_{Q_y}\right). \tag{5.71}$$

It is evident from Eq. (5.69) that the spin-wave spectrum is warped, i.e. it is dependent on the angular coordinate θ. The group velocity is

$$v_y = \frac{\partial\Omega_{\mathbf{q}}}{\partial q_y} = \frac{\left(J_1\xi_{Q_y} - 2J_2\xi_{Q_y} - 2D\bar{\xi}_{Q_y}\right)\Pi\, q_y}{\Omega_{\mathbf{q}}} \tag{5.72}$$

$$v_z = \frac{\partial\Omega_{\mathbf{q}}}{\partial q_z} = \frac{-\left(J_1 + 2J_2\xi_{Q_y}\right)\Pi\, q_z}{\Omega_{\mathbf{q}}} \tag{5.73}$$

where $\Pi = \left(-3J_1 + J_1\xi_{Q_y} - 2J_2\xi_{Q_y} - 2J_2 - 2D\bar{\xi}_{Q_y}\right)$. It is evident that the group velocity is different in the y and z directions. Consider now v_y at $q_z = 0$ and $J_2 = \frac{1}{2}|J_1|$

$$v_y = \frac{2\Delta_y q_y}{\sqrt{\Delta_y q_y^2}} = 2\sqrt{\Delta_y} = 2\sqrt{D\bar{\xi}_{Q_y}\left(4J_1 + 2D\xi_{Q_y}\right)}\,. \tag{5.74}$$

And consider similarly v_z at $q_y = 0$ and $J_2 = \frac{1}{2}|J_1|$

$$v_z = 2\sqrt{\Delta_z} = \sqrt{2J_1\left(1 + \xi_{Q_y}\right)\left(-4J_1 - 2D\bar{\xi}_{Q_y}\right)}\,. \tag{5.75}$$

Near the Γ-point the group velocities of the spin-waves excitations are constant in the y and z direction.

Chapter 6

Conclusion

In this thesis, the J_1-J_2 Heisenberg model on the two-dimensional square lattice was studied in detail. The ground state spin configuration has a highly frustrated point at $J_2 = \frac{1}{2}|J_1|$. The spin-wave dispersion was determined for all determinable ground state spin configurations of the model using local spin fluctuations and a Holstein-Primakoff transformation. The obtained dispersions were in agreement with each other and were considered in the limit of the highly frustrated point of the model. In this limit, the dispersion showed a spectrum of zero-energy modes. This suggests faulty assumptions in the calculation. The goal of this thesis was to investigate if additional interactions added to the system would yield an improved spin-wave dispersion.

The two-dimensional orthorhombic lattice was considered in the J_{1y}-J_{1z}-J_2 Heisenberg model. As a consequence of the geometry of the lattice, the exchange interaction, denoted J_1, in the square lattice is inherently different in the two axes of the orthorhombic lattice. This means that the system no longer has the highly frustrated point, and the degeneracy is therefore broken. The spin-wave dispersion was determined in all possible ground state spin configurations of the orthorhombic lattice and a reduction in zero-energy modes compared to the J_1-J_2 Heisenberg model on the square lattice could be seen.

Subsequently, the antisymmetric Dzyaloshinsky-Moriya interaction was added to the J_1-J_2 Heisenberg model on the two-dimensional square lattice. The ground state spin configuration was determined, and the additional interaction eliminated the highly frustrated point of the system. Spin-waves were introduced into the system, and both classical and quantum mechanical theories were used to obtain the spin-wave dispersions, which were once more in agreement with each other. The lines of zero-energy modes observed in the spin-wave dispersion of the J_2-J_1 Heisenberg model were removed with the addition of the Dzyaloshinsky-Moriya interaction. The group velocities of the low-energy modes were determined in the vicinity of the Γ-point.

To continue the work initiated in this thesis, one could add an external magnetic field and possibly a magnetic anisotropy to determine the effect that this would have on the ground state spin configuration and spin-wave dispersion. As only terms up to second order in the magnon operators were calculated in this thesis, the effect that higher order terms would have, such as magnon-magnon interactions and decays, could be interesting to explore.

Bibliography

[1] Q. Si and E. Abrahams, "Strong Correlations and Magnetic Frustration in the High T c Iron Pnictides," *Physical Review Letters*, vol. 101, p. 076401, Aug. 2008.

[2] P. W. Anderson, "The Resonating Valence Bond State in La2CuO4 and Superconductivity," *Science*, vol. 235, pp. 1196–1198, Mar. 1987.

[3] P. Chandra, P. Coleman, and A. I. Larkin, "Ising transition in frustrated Heisenberg models," *Physical Review Letters*, vol. 64, pp. 88–91, Jan. 1990.

[4] L. Wang and A. W. Sandvik, "Critical Level Crossings and Gapless Spin Liquid in the Square-Lattice Spin- 1 / 2 J 1 - J 2 Heisenberg Antiferromagnet," *Physical Review Letters*, vol. 121, p. 107202, Sept. 2018.

[5] Y. A. Kharkov, J. Oitmaa, and O. P. Sushkov, "Properties of the spin-liquid phase in the vicinity of the Lifshitz transition from Néel to spin-spiral state in frustrated magnets," *Physical Review B*, vol. 98, p. 144420, Oct. 2018.

[6] P. W. Anderson, "New Approach to the Theory of Superexchange Interactions," *Physical Review*, vol. 115, pp. 2–13, July 1959.

[7] I. Dzyaloshinsky, "A thermodynamic theory of "weak" ferromagnetism of antiferromagnetics," *Journal of Physics and Chemistry of Solids*, vol. 4, no. 4, pp. 241–255, 1958.

[8] T. Moriya, "Anisotropic Superexchange Interaction and Weak Ferromagnetism," *Physical Review*, vol. 120, pp. 91–98, Oct. 1960.

[9] F. J. dos Santos, M. dos Santos Dias, and S. Lounis, "Modeling spin waves in noncollinear antiferromagnets: Spin-flop states, spin spirals, skyrmions, and antiskyrmions," *Physical Review B*, vol. 102, p. 104436, Sept. 2020.

[10] X. Z. Yu, Y. Onose, N. Kanazawa, J. H. Park, J. H. Han, Y. Matsui, N. Nagaosa, and Y. Tokura, "Real-space observation of a two-dimensional skyrmion crystal," *Nature*, vol. 465, pp. 901–904, June 2010.

[11] H. M. Rønnow, D. F. McMorrow, and A. Harrison, "High-Temperature Magnetic Correlations in the 2D S = 1 / 2 Antiferromagnet Copper Formate Tetradeuterate," *Physical Review Letters*, vol. 82, pp. 3152–3155, Apr. 1999.

[12] M. P. Marder, *Condensed Matter Physics*. New York: John Wiley, 2000.

[13] J. Villain, "A magnetic analogue of stereoisomerism : Application to helimagnetism in two dimensions," *Journal de Physique*, vol. 38, no. 4, pp. 385–391, 1977.

[14] S. Blundell, *Magnetism in Condensed Matter*. No. 4 in Oxford Master Series in Condensed Matter Physics, Oxford: Oxford Univ. Press, reprint ed., 2014.

[15] S. H. Simon, *The Oxford Solid State Basics*. Oxford: Oxford University Press, 1st ed ed., 2013.

[16] T. A. Kaplan and N. Menyuk, "Spin ordering in three-dimensional crystals with strong competing exchange interactions," *Philosophical Magazine*, vol. 87, pp. 3711–3785, Sept. 2007.

[17] T. A. Kaplan, "Some Effects of Anisotropy on Spiral Spin-Configurations with Application to Rare-Earth Metals," *Physical Review*, vol. 124, pp. 329–339, Oct. 1961.

[18] A. Altland and B. Simons, *Condensed Matter Field Theory*. Cambridge ; New York: Cambridge University Press, 2nd ed ed., 2010.

[19] A. I. Akhiezer, V. G. Bar'yakhtar, and S. V. Peletminskii, *Spin Waves*, vol. 1 of *North-Holland Series in Low Temperature Physics*. 1968.

[20] T. Holstein and H. Primakoff, "Field Dependence of the Intrinsic Domain Magnetization of a Ferromagnet," *Physical Review*, vol. 58, pp. 1098–1113, Dec. 1940.

[21] C. L. Henley, "Ordering due to disorder in a frustrated vector antiferromagnet," *Physical Review Letters*, vol. 62, pp. 2056–2059, Apr. 1989.

[22] N. Arakawa, "Effects of magnon-magnon interactions in a noncollinear magnet induced by combination of a symmetric and an antisymmetric exchange interaction," *Physical Review B*, vol. 101, p. 064411, Feb. 2020.

[23] N. Arakawa and J.-i. Ohe, "Inplane anisotropy of longitudinal thermal conductivities and weak localization of magnons in a disordered spiral magnet," *Physical Review B*, vol. 98, p. 014421, July 2018.